Graduate Theses, Dissertations, and Problem Reports

2023

Modeling and Simulation of a Process That Converts Ethane to Ethylene and Ethylene to Low Density Polyethylene

Ernest Bosire Mokaya
ebmokaya@mix.wvu.edu

MODELING AND SIMULATION OF A PROCESS THAT CONVERTS ETHANE TO

ETHYLENE AND ETHYLENE TO LOW DENSITY POLYETHYLENE

Ernest Mokaya

Thesis Submitted

to the Statler College of Engineering and Mineral Resources

At West Virginia University

In Partial Fulfillment of the Requirements for the Degree of

Master's in

Chemical Engineering

Srinivas Palanki, Ph.D., Chair

Fernando Lima, Ph.D.

Yuhe Tian, Ph.D.

Department of Chemical and Biomedical Engineering

Morgantown, West Virginia

August 2023

ABSTRACT

MODELING AND SIMULATION OF A PROCESS THAT CONVERTS ETHANE TO ETHYLENE AND ETHYLENE TO LOW DENSITY POLYETHYLENE

Ernest Mokaya

Ethylene is a critical feedstock and a major building block in the petrochemical industry that is used in synthesizing important products like polyethylene, ethanol, ethylene oxide, ethylene dichloride and ethylbenzene. With increasing demand of plastics, production of ethylene and subsequently polyethylene has increased globally. This thesis conducts the modeling and simulation of an integrated process that utilizes ethane as the primary feedstock to produce ethylene and the subsequent polymerization of ethylene to low-density polyethylene (LDPE). The process combines two different processes into one integrated process: (1) conversion of ethane to ethylene and (2) conversion of ethylene to LDPE. First, a steady-state simulation for converting ethane gas from a shale gas processing plant into ethylene is developed and a sensitivity analysis with respect to variation in design operating conditions of different unit operations is performed. Second, a steady-state simulation for converting ethylene to LDPE is developed and a sensitivity analysis with respect to variation in design operating conditions of different unit operations and initiator concentration is performed. A heat integration approach for the whole process is utilized to minimize the utility costs and increase the efficiency of the process.

Dedication

To My Committee Members, Mother, and Sister,

I extend my sincere gratitude for your support and encouragement throughout this journey. Your contributions have been vital to my success, and I am grateful for your presence in my life.

To my esteemed committee members, thank you for your time and dedication in reviewing my work. Your valuable feedback and guidance have helped me refine my work and produce a better outcome. I appreciate your commitment to excellence and your belief in my potential.

To my dear mother, your unwavering belief in me has been a driving force behind my achievements. Thank you for always being my rock and providing the encouragement I needed to push forward. Your love and support mean the world to me.

To my supportive sister, thank you for standing by my side and cheering me on. Your words of encouragement and enthusiasm have motivated me to overcome challenges and strive for excellence. I am grateful for your constant support and understanding.

I recognize the impact each of you has had on my journey, and I want you to know that your contributions have not gone unnoticed. Your support has inspired me to persevere and reach new heights.

Thank You,

Ernest B. Mokaya

Table of Contents

<center>**Chapter 1**</center>

<center>**Manufacture of Ethylene and Low-Density Polyethylene**</center>

1.1 Introduction

Ethylene ($CH_2=CH_2$) is an olefin that is flammable, colorless, and has a sweet odor. It is an important feedstock and major building block in the petrochemical industry. Due to its reactive double bond chemical structure, ethylene is used as a raw material to produce industrial chemicals such as ethanol, ethylene oxide, ethylene dichloride and ethylbenzene. Ethylene can also be used as a feed stock to make numerous plastics products including Low Density Polyethylene (LDPE), Linear Low Density Polyethylene (LLDPE), and High Density Polyethylene (HDPE).

There are three common pathways to produce ethylene as mentioned below (Amghizar, et al. 2017).

- Steam cracking of hydrocarbons. This is the most common process for manufacturing ethylene. In this process, hydrocarbons such as naphtha, ethane, and propane are cracked with steam at temperatures ranging from 800 to 900°C to produce a mixture of ethylene and other products such as propylene and butadiene. The ethylene is then separated from the other products via distillation.

- Methanol-to-olefins (MTO). In this process, methanol can be converted to ethylene and other olefins over a catalyst. Methanol is catalytically produced from syngas that is a mixture of hydrogen and carbon monoxide. Syngas is sourced from natural gas or coal via Autothermal Reformation, Steam Methane Reformation or Partial Oxidation of the hydrocarbons.

- Catalytic dehydration of paraffins. In this process hydrogen is removed from the paraffins over a catalyst. The dehydrogenation reaction occurs at temperatures ranging from 500 to 700°C.

Ethylene plants in the United States have a capacity to produce over 1 million tons per year. Most plants utilize thermal cracking of hydrocarbons. The hydrocarbon feedstock mixed with steam enters the cracking section and is cracked into ethylene and various side products. The cracked gas enters the quench section and is cooled. Finally, the cooled gas enters a distillation train to be separated into a variety of desired final products. A variety of feedstocks can be used in a thermal cracking process. The feedstock for an ethylene plant can range from light paraffins such as methane, ethane, and propane to heavier paraffins.

With the popularization of hydraulic fracturing technology in the United States, many previously untapped shale gas deposits have become accessible. Because of this, the production of shale gas has significantly increased from 1% to 20% of total global production between 2000 and 2010 (Aruga, 2016). As shale gas contains ethane gas, an increase in shale gas production has also coincided with an increase in ethane gas production. The utilization system that will be considered in this research involves the conversion of ethane to ethylene and subsequent conversion of ethylene to LDPE.

1.2 Objective of Research

The overall objective of this proposal is simulation, analysis, and optimization of a process plant, which converts ethane gas to ethylene then ethylene to LDPE. The specific objectives are listed below:

- Develop a steady-state simulation for converting ethane gas into 72 tons/hr of 99.95 mol% polymer grade ethylene.

- Develop a steady-state simulation for converting ethylene into 15 tons/hr of 99.93 mol% low density polyethylene (LDPE).

- Develop a heat integration approach for the whole process to minimize the utility costs and increase the efficiency of the process.

1.3 Significance of Research

Shale gas production in the United States has seen a significant increase over the past decade. Advances in drilling techniques, such as hydraulic fracturing and horizontal drilling, have made it possible to extract natural gas from shale gas deposits that were previously inaccessible. This has led to significant increase in ethane production within the United States. According to the Unites States Energy Information Administration, ethane production is expected to increase from 2.2 million barrels per day in 2021 to over 3 million barrels per day by 2050 (Wilczewski and Eiermann 2022). As a result of increased ethane production, the production of ethylene has also increased. Ethylene can be further processed to produce polyethylene. Due to increasing global demand of plastics, it is projected that the production of polyethylene has increased. According to the American Chemistry Council, the production of polyethylene in the United States has increased from 13.2 million metric tons in 2000 to 22.7 million metric tons in 2019 and the growth rate is expected to be 2.6% per year until 2024 (American Chemistry Council 2020). Because of increased demand of various plastic products made from polyethylene, it is valuable to conduct a study and analysis on the conversion of ethane to ethylene to polyethylene to reduce both capital cost and operating cost.

Chapter 2
Literature Survey

2.1 Shale Gas Overview

Shale gas is a type of natural gas that is trapped inside shale rock formations. The shale rock formations are of fine sedimentary rock composed of clay minerals and other small organic particles. Within the United States there are three major shale rock formations listed below:

- The Marcellus shale formation, which is one of the largest formations in the world spanning from West Virginia through Pennsylvania and parts of Ohio, and into New York. A key feature of the shale formation is that has low levels of sulfur dioxide, nitrogen oxide, carbon monoxide and mercury (Kargbo, Wilhelm and Campbell 2010).

- The Bakken shale formation, which spans from North Dakota into parts of Montana and Canada. A key feature of this shale formation is the availability of both oil in the form of oil sands and natural gas (Grape 2010).

- The Barnett shale formation, which is in north central Texas. The shale formation was one of the first to be accessed through hydraulic fracturing and horizontal drilling technology (Martineau 2007).

Shale formations have low permeability due to tiny and poorly connected pore spaces. To access natural gas inside the formations traditional vertical drilling cannot be utilized so new drilling technology and techniques have been developed. To access the natural gas reserves in shale formations, a combination of both hydraulic fracturing and horizontal drilling technology is employed. Before drilling is done, an initial exploration of possible gas deposits is done by conducting geologic, seismic, and petrophysical surveys. Once a gas deposit is identified, pre-drilling is performed to confirm the location of the gas deposit and analyze the shale rock

formation. Following the initial exploration, a well is drilled vertically with the well bore trajectory gradually becoming horizontal to access the gas deposit. To prevent the contamination of surrounding ground water metal casings and cement are simultaneously deposited as the well is being drilled by creating a pressure barrier. Once the well is completed, a perforation gun shoots holes through the casings and cement at set intervals to create fractures along the shale formation to connect the gas deposit to the well bore. Subsequently, a mixture of water, sand, and chemicals are pumped into the well to increase the amount of released natural gas (Kargbo, Wilhelm and Campbell 2010).

2.2 Shale Gas Composition

Shale gas is a natural gas that is primarily composed of methane in addition to other hydrocarbons, such as ethane, propane, and butane, as well as trace amounts of inorganics such as nitrogen, carbon dioxide, and hydrogen sulfide. Many studies have analyzed the composition of shale gas from the Marcellus formation in the United States. It has been found that the shale gas from this formation is predominantly composed of methane, with an average methane content ranging from 94.45 to 97.87 mol%. Ethane, propane, and butane accounted for the remaining hydrocarbons, with ethane being the most abundant (Laughrey 2022).

Overall, the composition of shale gas can vary depending on the shale rock formation and other factors, but it is primarily composed of methane, with smaller amounts of other hydrocarbons and trace gases. This is displayed in Table 2.1, which shows typical natural gas composition.

Table 2.1: Typical Natural Gas Composition (Speight, The Chemistry and Technology of Petroleum - 5th Edition 2013)

Component	Volume %
Methane	>85
Ethane	3 - 8
Propane	1 - 5
Butane	1 - 2
Pentane	1 - 5
Carbon Dioxide	1 - 2
Hydrogen Sulfide	1 - 2
Nitrogen	1 - 5
Helium	<0.5

2.3 Shale Gas Processing

Shale gas processing is a complex and multi-step process that involves separating the natural gas from other substances, such as water and impurities, before it can be transported and used as a feedstock for production facilities or fuel to heat homes. During gas processing, the shale gas is first treated to remove impurities, such as water, carbon dioxide, and hydrogen sulfide. The first section of a shale gas processing facility is typically acid gas removal unit that is used to remove carbon dioxide and hydrogen sulfide via an amine scrubber. Sweetened gas then enters a dehydration unit where water is removed from the natural gas via a glycol dehydrator. Once dehydrated, the natural gas is cooled and enters a de-methanizer where the gas is cryogenically distilled to separate methane from heavy paraffins also known as natural gas liquids (NGL). The NGLs are fed into a fractionation train where they are separated into ethane, butane and other heavier paraffins (Luo and Fengqi 2018). This whole sequence of processing steps is shown in Figure 2.1.
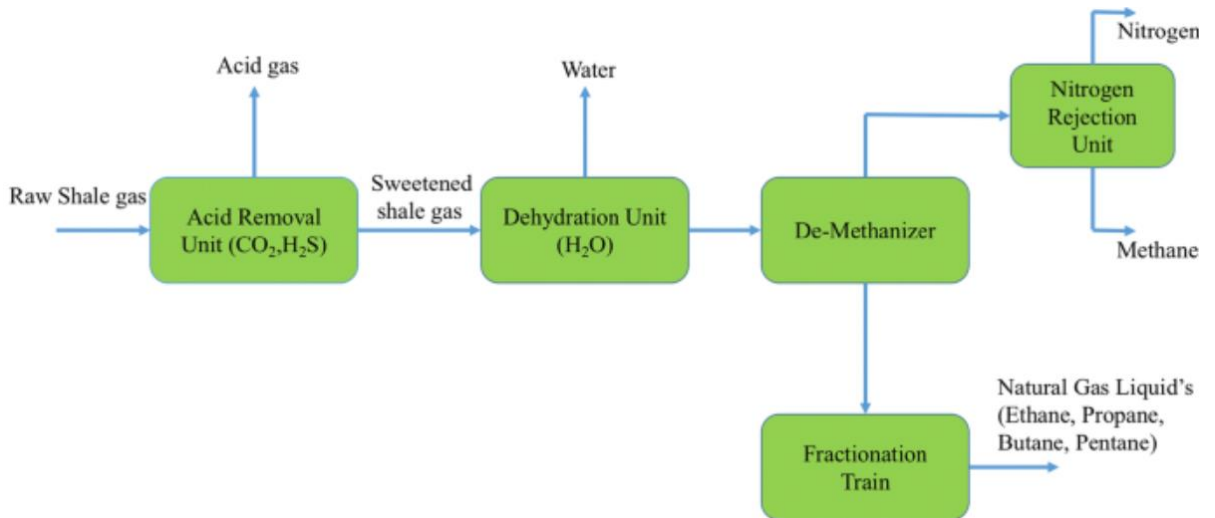
Figure 2.1 Shale Gas Processing Block Flow Diagram. Adapted from (Asani, Mukherjee and El-Halwagi 2020))

2.4 Ethane to Ethylene

Thermal Steam Cracking

Thermal stream cracking of paraffins is the most common method employed to produce light paraffins. Currently, 95% of global ethylene production and 60% of global propylene production is produced using this method (Sadramel 2016). In a thermal cracking process, the feedstock can range from light paraffins such as ethane and propane to heavy hydrocarbons like naphtha, n-pentane, n-hexane. The choices of the feedstocks depend on feed availability and process economics. The thermal stream cracking reaction is highly endothermic taking place in a

furnace with multiple tubes of plug flow reactors. When ethane is used as the feedstock, the following reactions occurs:

$$C_2H_6 \leftrightarrow C_2H_4 + H_2$$

$$C_3H_6 \leftrightarrow C_2H_2 + CH_2$$

$$C_2H_2 + C_2H_4 \rightarrow C_4H_6$$

$$C_2H_4 + C_4H_6 \rightarrow C_6H_6 + 2H_2$$

$$C_3H_8 \leftrightarrow C_3H_6 + H_2$$

$$C_3H_8 + C_2H_4 \rightarrow C_2H_6 + C_3H_6$$

$$2C_3H_8 \rightarrow 2C_2H_4$$

$$2C_2H_6 \rightarrow C_3H_8 + CH_4$$

$$C_4H_{10} \leftrightarrow C_4H_8 + H_2$$

$$C_2H_4 + C_2H_6 \rightarrow C_3H_6 + CH_4$$

$$C_3H_6 + C_2H_6 \rightarrow C_4H_8 + CH_4$$
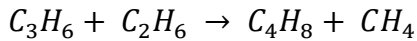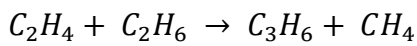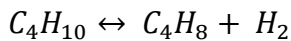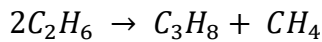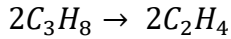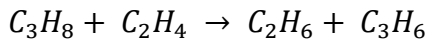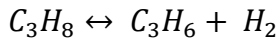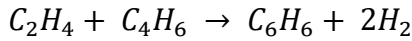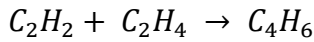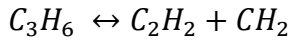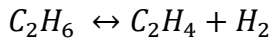
The steam to hydrocarbon ratio is maintained between 0.3 and 0.5 by mass. With ethane being one of the most stable feedstocks, to produce ethylene the reactor operates at a temperature between 800 °C and 900 °C and a pressure between 1 – 3 atm (Ranjan, et al. 2012). Before to entering the reactor, ethane is preheated in the convection section of the furnace, and then mixed with superheated steam at a predetermined steam to hydrocarbon ratio. The mixed feed then enters the radiant section where the reactor is housed, and the thermal steam cracking reaction occurs. Effluent from the radiant section is cooled rapidly by a Transfer Line Exchanger (TLE) to below reaction temperature to stop any reactions and then sent to a distillation train to separate C1, C2, and C3+ products. Unreacted feed is recycled back into the reactor while methane and other undesired products are used as fuel gas (Rosli and Aziz 2016). Figure 2.2 displays the typical

schematic of a steam cracking furnace and figure 2.3 shows a block flow diagram of an ethylene production plant.
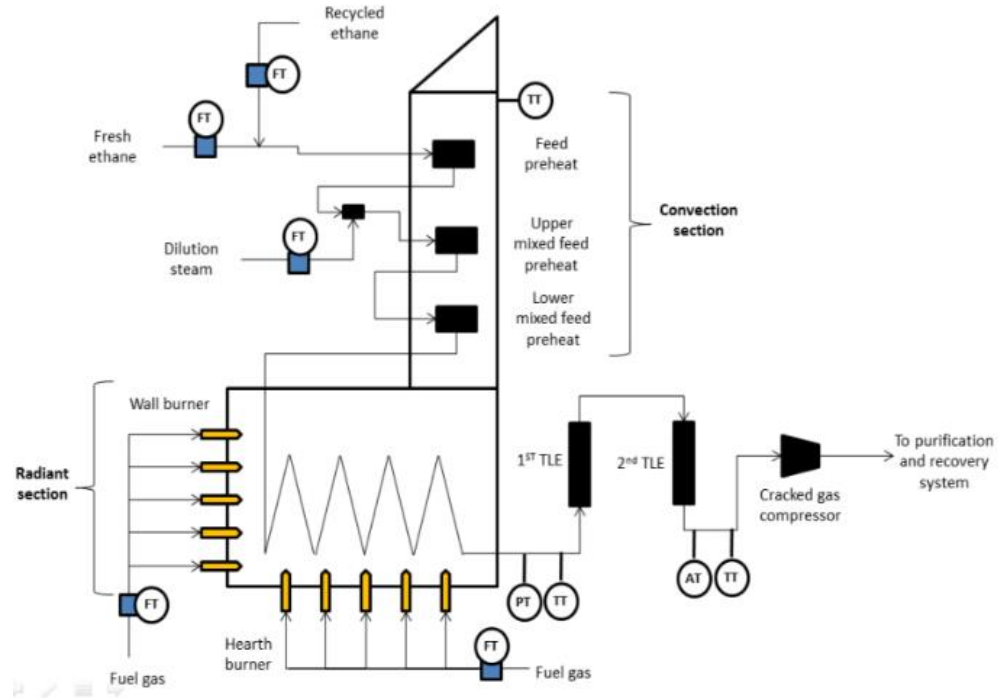
Figure 2.2: Schematic of ethane steam cracking furnace. Adapted from (Rosli and Aziz 2016)
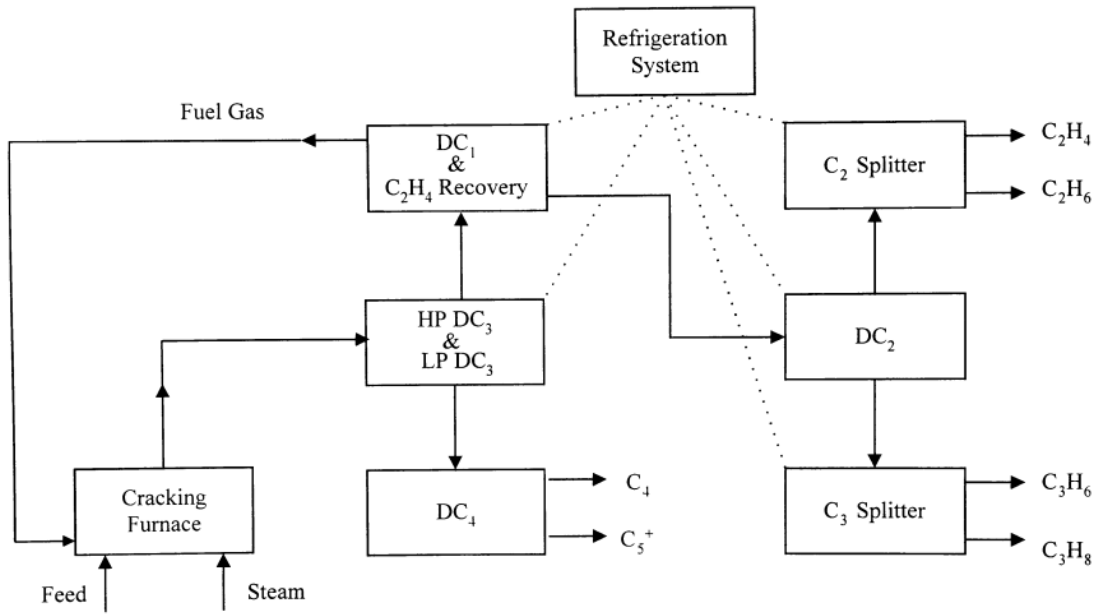
Figure 2.3: Process flowsheet for an ethylene plant

Fluidized Catalytic Cracking (FCC)

An alternative technology employed to of produce ethylene is through fluidized catalytic cracking (FCC). FCC units are very flexible units where the feedstock can range from light paraffins to heavy hydrocarbons. The component within the FCC unit that causes it to fluidize is the micro spherical catalyst ranging from 60μm to 80μm in diameter that fluidizes when air is forced into the catalyst bed by an air blower (Sadeghbeigi 2020). The feedstock for an FCC unit is most often heavy gas oil but light paraffins can be used as an alternative to produce light olefins.

There are 5 major components in an FCC unit, which are the catalyst, riser, reactor, regenerator, and fractionator. The feed stock is mixed with steam then fed into the riser where it is mixed with the regenerated catalyst. The riser then feeds into the reactor where product vapors is separated from spent catalyst via a cyclone or disengaging device. Product vapors are separated out into different components in the fractionator while the spent catalyst falls into a stream stripper where it is un-clumped before entering the regenerator. Inside the regenerator, the catalyst is regenerated by burning the built-up coke. Figure 2.4 shows the schematic for a typical FCC unit.
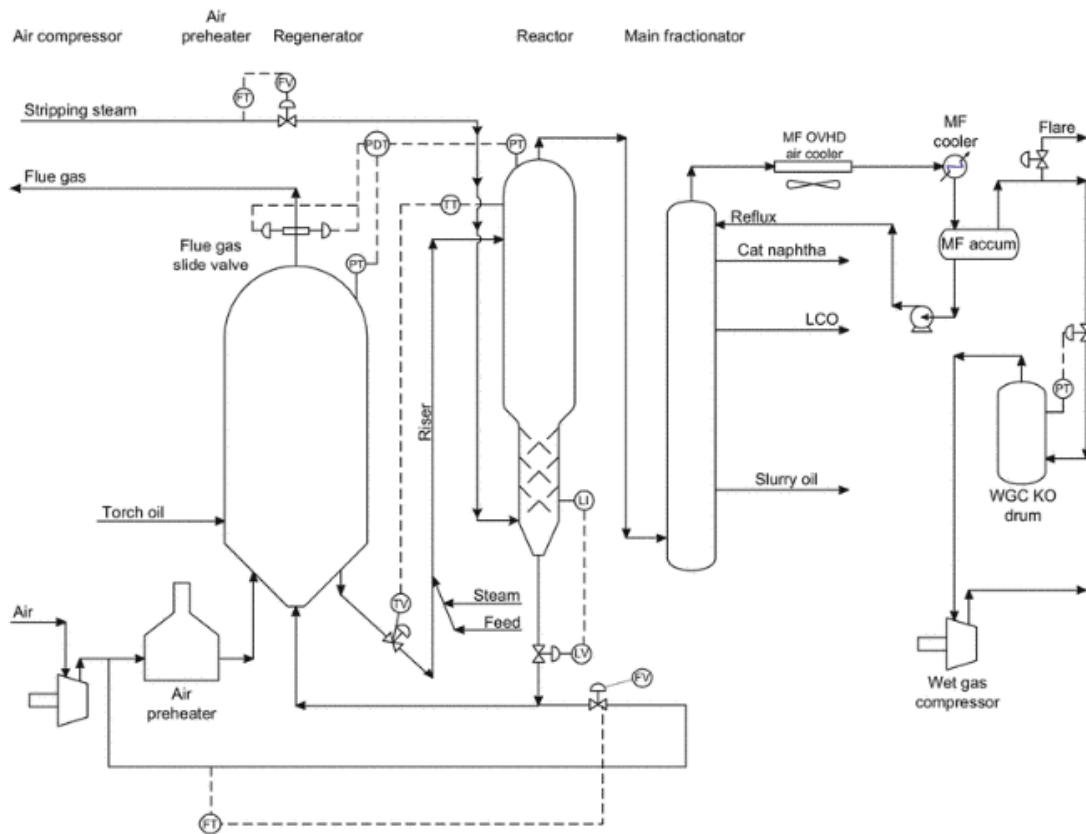
Figure 2.4: Process Flow Diagram of FCC Unit. Adapted from (Sadeghbeigi 2020)

When the feed stock – steam mixture enters the riser, the catalytic reaction immediately begins when the feed is vaporized. In modern FCC units, the riser operates as the primary reactor while the reactor operates to separate the product from the catalyst. The operating temperature of the reactor and riser range from 496°C to 565°C and a pressure ranging from 1 to 3 bars (Sadeghbeigi 2020).

The reaction that takes place within the FCC unit is endothermic and is summarized as the cracking of straight chain paraffins into smaller paraffins, olefins, and aromatics. The catalytic cracking reaction follows an ionic reaction mechanism. The mechanism begins when the regenerated catalyst meets the feed, the feed is vaporized resulting in a positively charged carbon ion called Carbonium CH_5^+ or Carbenium R- CH_2^+. The Carbonium ion is formed by adding a

hydrogen atom (H$^+$). Carbenium forms form either adding a positive charge to an olefin or from removing a hydrogen and two electrons from a paraffin. The carbon ion is then cracked to produce an olefin and a new Carbenium ion. The Carbenium ion is only depleted when two ions collide forming a paraffin (Sadeghbeigi 2020). Figure 2.4 displays a simplified catalytic cracking mechanism of hydrocarbons and figure 2.5 shows a summary of the ionic reaction mechanism.
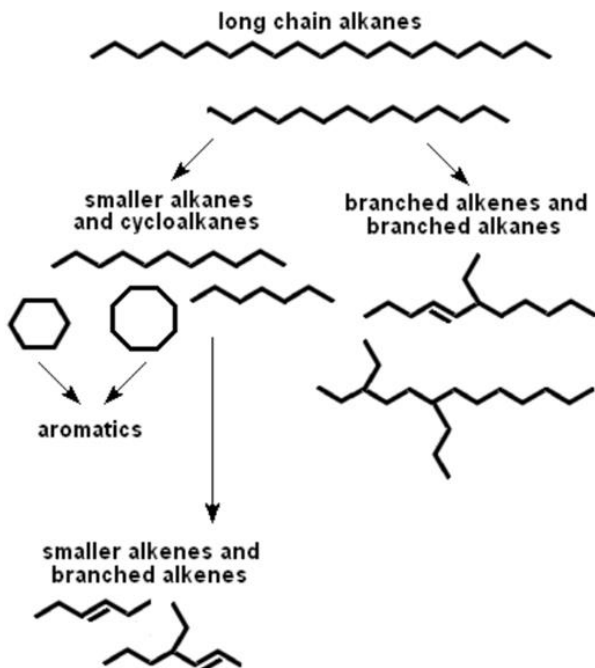
Figure 2.5: Example of the Catalytic Cracking of Petroleum Hydrocarbons. Adapted from (Speight, The Chemistry and Technology of Petroleum - 4th Edition 2006)

Carbonium Formation
R-CH$_2$-CH$_2$-CH$_2$-CH$_3$ + H$^+$ (proton attack) $\rightarrow$ R-C$^+$H-CH$_2$-CH$_2$-CH$_3$ + H$_2$
Carbenium Formation
R$-$CH $=$ CH$-$CH$_2$$-CH_2$$-CH_3$ + H$^+$ (a proton @ Bronsted site) $\rightarrow$
R$-$C$^+$H$-$CH$_2$$-CH_2$$-CH_2$$-CH_3$

R$-$CH$_2$$-CH_2$$-CH_2$$-CH_3$ (removal of H$^-$ @ Lewis site) $\rightarrow$ R$-$C$^+$H$-$CH$_2$$-CH_2$$-CH_3$
Cracking Reaction
R$-$C$^+$H$-$CH$_2$$-CH_2$$-CH_2$$-CH_3$ $\rightarrow$ CH$_3$$-$CH $=$ CH$_2$ + C$^+$H$_2$$-CH_2$$-CH_2$R
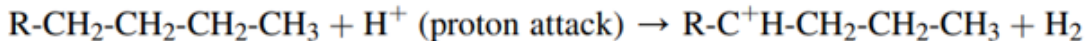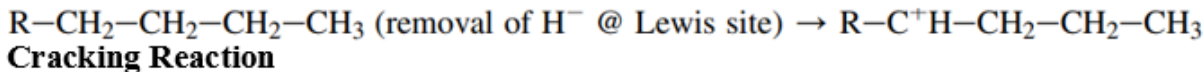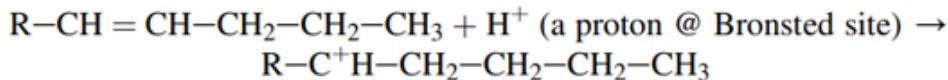
Figure 2.6: Catalytic Cracking Ionic Reaction Mechanism. Adapted from *(Sadeghbeigi 2020)*

The major issue with catalytic cracking is the formation of coke on the catalyst. Coking occurs when hydrocarbon vapors fill up and plug the catalyst pores with carbon. Coking of the catalyst leads to the catalyst deactivation and clumping. A catalyst steam stripper is employed to separate the catalyst before entering the regenerator. Within of the regenerator catalyst activity is restored and all the necessary heat for the cracking reaction is produced. To restore catalyst activity, the built-up coke is burned off the catalyst. The necessary oxygen for the reaction is fed to the regenerator through an air blower then dispersed evenly by an air distributor. The air distributor also functions to fluidize the regenerator bed. The regenerator operates at temperatures ranges from 677°C to 792°C and pressures ranging from 1 to 3 bars (Sadeghbeigi 2020). Figure 2.7 displays the combustion reaction that occurs in a regenerator.

$$C + \tfrac{1}{2}\,O_2 \rightarrow CO$$
$$CO + 1/2\,O_2 \rightarrow CO_2$$
$$C + O_2 \rightarrow CO_2$$
$$H_2 + 1/2\,O_2 \rightarrow H_2O$$
$$S + xO \rightarrow SO_X$$
$$N + xO \rightarrow NO_X$$
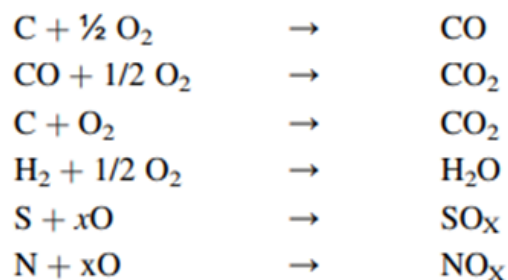
Figure 2.7: Combustion of Coke. Adapted from (Sadeghbeigi 2020)

Downstream from the FCC unit is a fractionator that is used to separate the different components within the product gas. The fractionator can be either a distillation column or a packed bed column. In industry it is typically a distillation column for easier removal of side products. Light olefins from the unit can be further distilled to recover ethylene.

2.5 Ethylene to Polyethylene

Polyethylene is a type of plastic that is widely used in many applications due to its versatility, durability, and low cost. It is a thermoplastic polymer meaning that it can be melted and reprocessed many times at high temperature while maintaining mechanical and physical

13

properties. Polyethylene is made from ethylene monomer units and is produced in different forms including high-density polyethylene (HDPE), low-density polyethylene (LDPE), and linear low-density polyethylene (LLDPE). HDPE has a high strength-to-density ratio and is used in a variety of products, including plastic bags, milk jugs, and detergent bottles. LDPE is flexible and used in products such as squeezable bottles and plastic wrap. LLDPE has a higher tensile strength and is used in applications such as packaging films and liners (Spalding and Chatterjee 2018). HDPE and LLDPE both have short-chain branches and have a density of 0.93 – 0.97 g/ml and 0.91 – 0.93 g/ml respectively. LDPE has long-chain branches and has a density of 0.91 – 0.93 g/ml (Xie, et al. 1994). Figure 2.8 displays the molecular structure of the three different types of polyethylene.
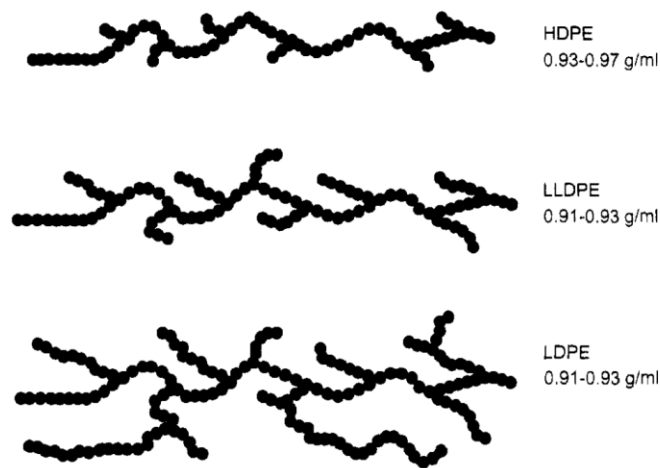
Figure 2.8: Molecular structure of commercial polyethylene. Adapted from (Xie, et al. 1994)

Ethylene to Low Density Polyethylene (LDPE)

Conversion of ethylene to Low Density Polyethylene (LDPE) is done through the free radical polymerization reaction of ethylene which is initiated by oxygen and peroxides. The reaction takes place within a tubular reactor that operates at temperatures ranging from 130°C to 300 °C and pressures ranging from 1200 bar to 3000 bar. With the polymerization reaction being

highly exothermic, high-pressure water is run through the jacket of the reactor to cool the reactor and prevent the crystallization of LDPE on the reactor walls (Spalding and Chatterjee 2018).

The simple free radical polymerization of ethylene is composed of the four following reactions: initiator decomposition, chain initiation, chain propagation, and chain termination. In the initiator decomposition reaction, the initiator is broken down to form free radicals which are an intermediate with an unpaired electron. Following the decomposition of the initiator, the chain initiation reaction occurs in which the free radicals react with ethylene monomers to form polymer radicals. Subsequently, the chain propagation reaction occurs where the polymer radicals react with ethylene monomers to form longer polymer chains. To stop the polymerization reaction, the chain termination reaction takes place where two polymer radicals merge or form two dead polymer chains (Muhammad, Ahmad and Aziz 2021).

In a high-pressure polyethylene production process, fresh ethylene together with recycled ethylene and initiator is compressed to reactor operating pressure and then mixed with the initiator. Following the compression stage, the mixture of ethylene and initiator is fed into a two-zone reactor where the free radical polymerization reaction occurs to form LDPE. Reactor product is then fed to a high-pressure and low-pressure separator to separate LDPE from unreacted ethylene and drop the pressure to 0.5 bar. Unreacted ethylene is recycled back into the reactor and the LDPE

is sent to an extruder where it is further degassed and pelletized (Spalding and Chatterjee 2018).

Figure 2.9 displays a high-pressure tubular reactor used for the manufacturing of LDPE.
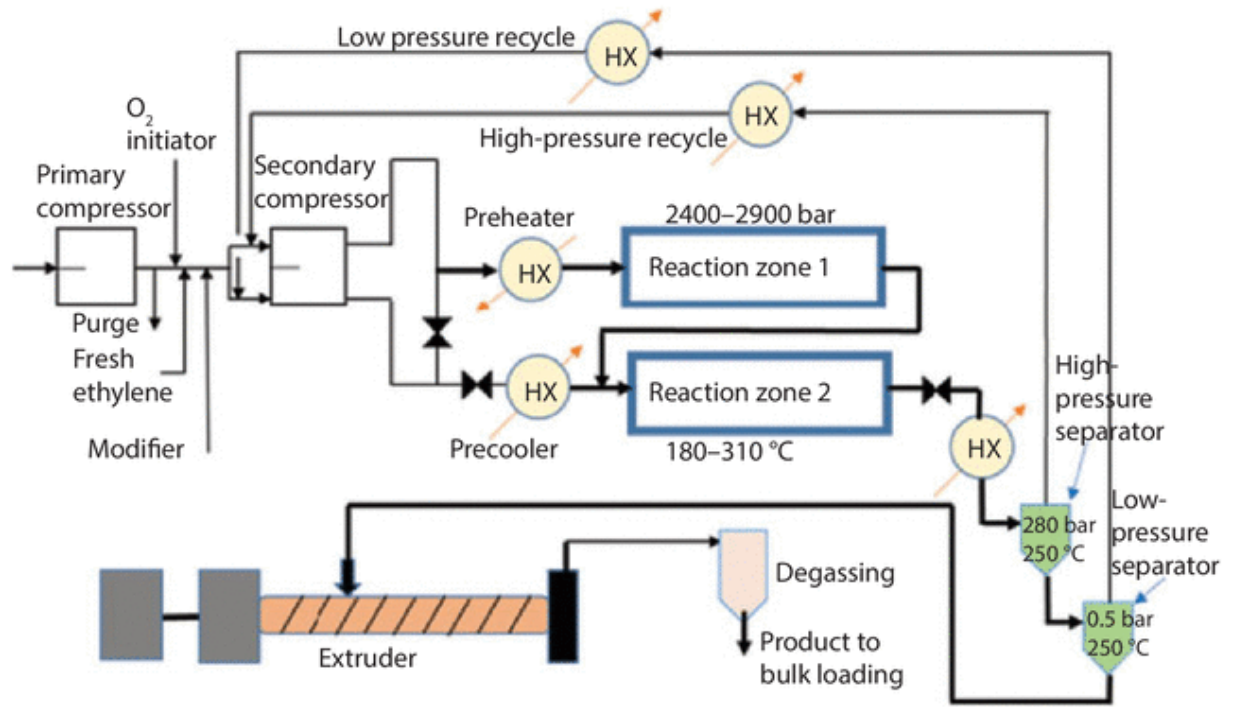
Figure 2.9: High-pressure tubular process to produce LDPE. Adapted from (Spalding and Chatterjee 2018)

Ethylene to Linear Low-Density Polyethylene (LLDPE) and High-Density Polyethylene (HDPE)

Conversion of ethylene to linear low-density polyethylene (LLDPE) and high-density polyethylene (HDPE) can be achieved in a gas-phase fluidized bed reactor by utilizing different catalysts. To produce HDPE a Phillips chromium-oxide catalyst is used and to produce LLDPE, a Zeigler-Natta catalyst is used. Common Zeigler-Natta catalysts include titanium tetrachloride ($TiCl_4$) and trimethylaluminum ($Al(C_2H_5)_3$) (Alves, et al. 2021). Within the fluidized bed reactor, the exothermic reactions shown in Table 2.2 place.

Table 2.2: Summary of Elementary Reactions for Ethylene Copolymerization. Adapted from (Alves, et al. 2021)

Site activation	$S_p^k + AlR_3 \xrightarrow{k_a^k} P_0^k$	Conversion of inactive potential catalyst sites, S_p^k, to reactive vacant sites, P_0^k. Activation commonly occurs by reaction of a potential site with a cocatalyst (AlR_3).
Chain initiation	$P_0^k + M_i \xrightarrow{k_{0i}^k} P_{1,i}^k$	A monomer molecule of type i, M_i, reacts with an activated vacant site, producing an active site occupied by a chain made of a single monomer, $P_{1,i}^k$.
Chain propagation	$P_{n,1}^k + M_i \xrightarrow{k_{p1i}^k} P_{n+1,i}^k$	Main polymerization reaction step. The active chain of length n and with a monomer of type j at the active site, $P_{n,j}^k$, reacts with a monomer molecule of type i, increasing its chain length by one, $P_{n+1,i}^k$
	$P_{n,2}^k + M_i \xrightarrow{k_{p2i}^k} P_{n+1,i}^k$	
Chain transfer To hydrogen To co-catalyst To monomer Spontaneous	$P_{n,i}^k + H_2 \xrightarrow{k_{tH,i}^k} P_H^k + D_n^k$	These reactions terminate the growth of live polymer chains, forming dead polymer chains, D_n^k, and vacant active sites, P_0^k, or $P_{1,j}^k$. Termination by hydrogen is thought to lead to a dormant site P_H^k.
	$P_{n,i}^k + A \xrightarrow{k_{tA,i}^k} P_0^k + D_n^k$	
	$P_{n,i}^k + M_j \xrightarrow{k_{tj,i}^k} P_{1,j}^k + D_n^k$	
	$P_{n,i}^k \xrightarrow{k_{tSP,i}^k} P_0^k + D_n^k$	
Dormant site reactivation	$P_H^k + M_i \xrightarrow{k_{Hi}^k} P_{1,i}^k$	A monomer molecule, M_i, reacts with a dormant site, producing an active site occupied by a single monomer, $P_{1,i}^k$. The reactivation rate constant (k_{Hi}^k) is smaller than the value of k_{0i}^k
Site deactivation By hydrogen By co-catalyst By monomer Spontaneous	$P_{n,i}^k + H_2 \xrightarrow{k_{bH,i}^k} C_D^k + D_n^k$	Deactivation reactions form dead sites, C_D^k and dead polymer chains. Typically, spontaneous deactivation predominates, but deactivation by other means, such as poisoning reactions with polar impurities present in the reactor, is also possible.
	$P_{n,i}^k + A \xrightarrow{k_{bA,i}^k} C_D^k + D_n^k$	
	$P_{n,i}^k + M_j \xrightarrow{k_{bi,j}^k} C_D^k + D_n^k$	
	$P_{n,i}^k \xrightarrow{k_{bSP,i}^k} C_D^k + D_n^k$	

The fluidized bed reactor operates at temperatures ranging from 70°C to 120°C and pressures ranging from 20 to 30 bar. The polymerization process begins activated catalyst particles encounters compressed ethylene, a co-monomer, and hydrogen. The gaseous species are transported to the catalyst active sites and begin to polymerize. Polymer subsequently begins to build up on the catalyst surface with the size of the catalyst particle increasing to 200 – 1000 µm. Large polymer particles are recovered from the fluidized bed reactor and separated from the catalyst. The polymer is finally sent to an extruder and pelletized. All the heat produced in the polymerization process is removed by the cycle gas, which is then recycled into the reactor after it is cooled down by a cold-water heat exchanger. The feed and recycled cycle gas also function to fluidize the reactor bed. ((Spalding and Chatterjee 2018), (Xie, et al. 1994)). Figure 2.10 shows a diagram of a common fluidized bed reactor.
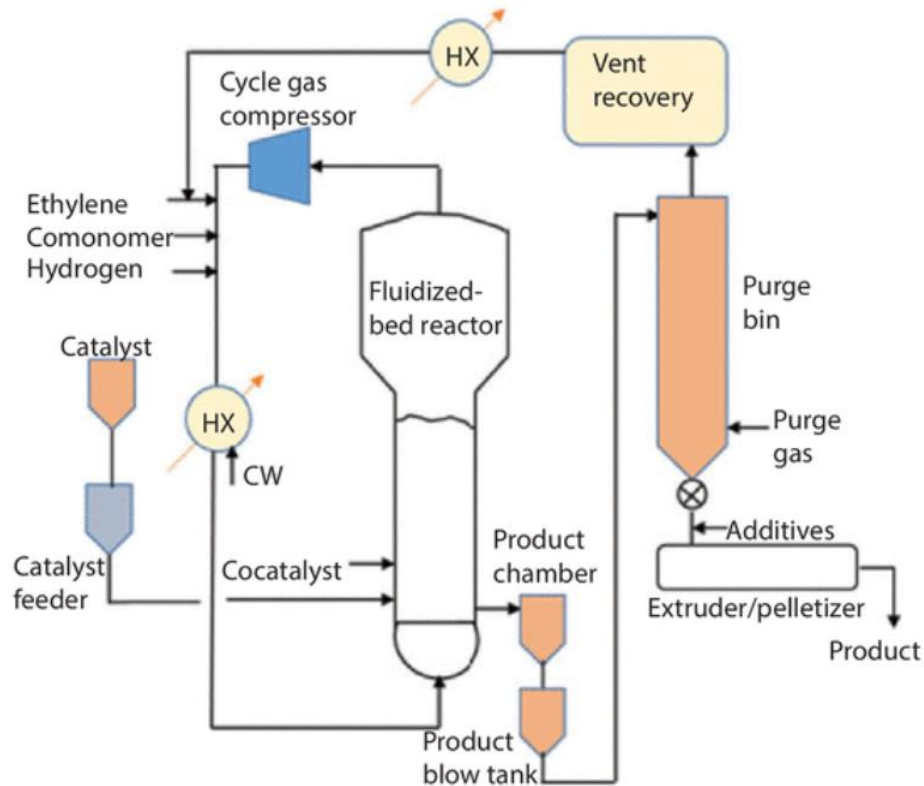
Figure 2.10: Diagram of a gas-phase fluidized bed reaction system licensed by Univation Technologies. Adapted from (Spalding and Chatterjee 2018)

2.6 Heat Integration Technology

Previous literature has shown that currently, there are separate process plants that can convert ethane to ethylene, ethylene to polyethylene. The objective of this research is to consider an integrated plant that utilizes ethane to produce polyethylene. A major advantage of considering an integrated plant is that it is possible to utilize heat integrating technology, to reduce the cost of hot and cold utilities. In particular, the use of a heat exchanger network (HEN) will be considered. The optimization of HEN is based on the objective function of minimizing the total utility costs and the minimum temperature approach ΔT_{min} adopted is 1 °C.

To optimize the heat exchanger units, heat exchange area and loads on each utility a mixed-integer-linear-programming (MILP) approach is often used. To calculate the fitness the δ function is used. δ is defined as:

$$\delta_{ijk} = \left| 1 - \left| \frac{q_{ijk}}{Q_k} \frac{\frac{1}{CP_i} - \frac{1}{CP_j}}{\frac{1}{CP_{(Hot-quasi)k}} - \frac{1}{CP_{(Cold-quasi)k}}} \right| \right|; \text{ when } CP_{(Hot-quasi)k} \neq CP_{(Cold-quasi)k} \tag{1}$$

and

$$\delta_{ijk} = \frac{q_{ijk}}{Q_k} \frac{CP_{(Hot-quasi)k}}{CP_i} \left| 1 - \frac{CP_i}{CP_j} \right|; \quad \text{when } CP_{(Hot-quasi)k} = CP_{(Cold-quasi)k} \tag{2}$$

where,

CP_i = the heat capacity flowrate of hot stream i,

CP_j = the heat capacity flowrate of cold stream j,

q_{ijk} = the heat load between hot stream i and cold stream j in k[th] block

Q_k = enthalpy change of kth block

$CP_{(Hot-quasi)k}$ = the heat capacity flowrate of the hot quasi-composites in k[th] block

$CP_{(Cold-quasi)k}$ = the heat capacity flowrate of the cold quasi-composites in k[th] block

The optimum HEN design can be found by minimizing an objective function defined as:

$$minimize \sum_{ij} \delta_{ij} \tag{3}$$

The minimization problem is formulated as MILP. In the problem, hot and cold streams of equal number (n) are studied. δ_{ij} is defined as the fitness to the quasi-composites by a match between hot stream i and cold stream j. The binary variables x_{ij} indicates the existence of a match between hot stream i and cold stream j, i.e. $x_{ij} = 0$ non-existence of a match and $x_{ij} = 1$ declares the existence of a match . Using the defined variables, equation (3) can be converted to the following MILP problem:

$$minimize \sum_{i,j=1}^{n} \delta_{ij} . x_{ij}$$

$$\sum_{i=1}^{n} x_{ij} = 1 \quad j = 1, ... , n$$

$$\sum_{j=1}^{n} x_{ij} = 1 \quad i = 1, ... , n$$

$$x_{ij} = 0, 1 \quad i, j = 1, ... , n \tag{4}$$

This method considers both minimization of both overall surface area using the δ function and the number of units. It should be noted that the MILP model always gives the best set of matches rather than a single match. If the total number of hot streams and cold streams are not equal, dummy elements with zero assignment are added to make matrix square and then MILP model can be applied (Zhu 1997).

2.7 Conclusions

This literature survey indicates that there are no comprehensive simulation studies that utilize a systematic approach for the development of an integrated plant that produces low density polyethylene from ethane. Furthermore, heat integration for this integrated plant have not been performed. With the increasing economic importance of producing polyethylene from ethane, it is necessary to find ways to minimize both operating cost and capital cost of this plant.

Chapter 3

Steady State Simulation to Convert Ethane Gas to Ethylene and Ethylene to Low Density Polyethylene

3.1 Process Description

The research study investigates the feasibility of developing a steady state process for manufacturing low density polyethylene (LDPE) from ethane. Figure 3.1 show the block flow diagram for the process used to covert ethane to LDPE with ethylene being the intermediate product.
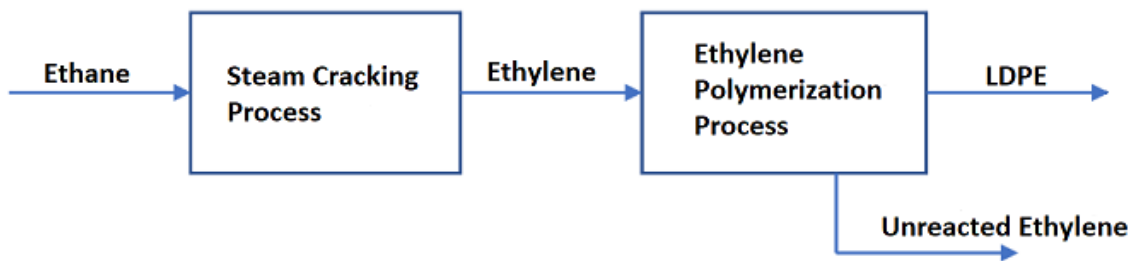
Figure 3.11. Block diagram to Produce LDPE from Ethane

The LDPE manufacturing process is divided into 2 sub-plants: (1) conversion of ethane to ethylene, and (2) conversion of ethylene to LDPE. Figure 3.2 shows the process flow diagram of the entire process, and the process is further discussed below.

Figure 3.12. Process flow diagram from Ethane to Ethylene and Ethylene to LDPE

The ethylene production process utilized in this research is the thermal steam cracking of ethane gas described in literature (Rosli and Aziz 2016). The feed to the production process is ethane gas that comes from an ethane gas pipeline. Fresh ethane gas is fed into the process at a rate of 108 tons/hr and mixed with 41 tons/hr recycled ethane. The ethane gas is mixed with 50 tons/hr of process steam to achieve a steam to hydrocarbon ration of 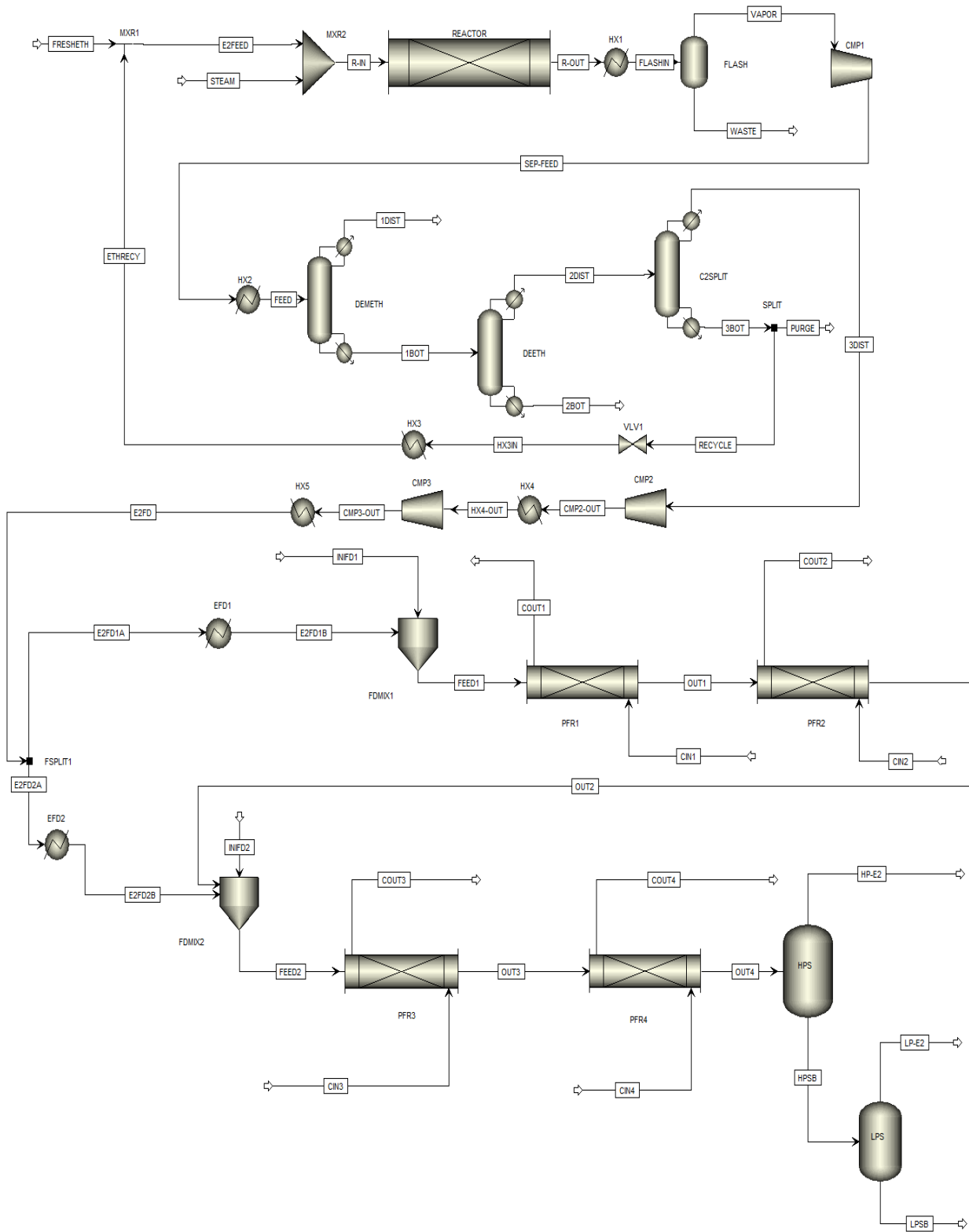0.33 by mass and passed through the thermal stream cracking reactor at 700 °C and 3.2 bar. The reaction conditions are 840 °C and 3.2 bar for the reactor. At these conditions, the thermal steam cracking reaction occurs where the ethane feed stock is converted to a gas containing mostly ethylene, methane, hydrogen, and residual ethane. The reaction kinetics are shown below in Table 3.1.

Table 3.1. Ethane Cracking Power Law Reaction Kinetics (Rosli and Aziz 2016)

No	Reaction	Order	Forward Reaction		Reverse Reaction	
			A [s^{-1}] or [L (mol s)$^{-1}$]		A [L (mol s)$^{-1}$]	
			E [kJ mol^{-1}]		E [kJ mol^{-1}]	
1	$C_2H_6 \leftrightarrow C_2H_4 + H_2$	1	$A = 4.6 \times 10^{13}$	$E = 272.8$	$A = 8.49 \times 10^8$	$E = 136.5$
2	$C_3H_6 \leftrightarrow C_2H_2 + CH_4$	1	$A = 7.2 \times 10^{12}$	$E = 274.2$	$A = 3.81 \times 10^8$	$E = 147.2$
3	$C_2H_2 + C_2H_4 \rightarrow C_4H_6$	2	$A = 1.0 \times 10^{15}$	$E = 172.6$		
4	$C_2H_4 + C_4H_6 \rightarrow C_6H_6 + 2H_2$	2	$A = 8.3 \times 10^{12}$	$E = 144.6$		
5	$C_3H_8 \leftrightarrow C_3H_6 + H_2$	1	$A = 5.8 \times 10^{10}$	$E = 214.6$	$A = 9.03 \times 10^5$	$E = 93.5$
6	$C_3H_8 + C_2H_4 \rightarrow C_2H_6 + C_3H_6$	2	$A = 2.5 \times 10^{16}$	$E = 247.1$		
7	$2C_3H_6 \rightarrow 3C_2H_4$	1	$A = 7.3 \times 10^{12}$	$E = 268.5$		
8	$2C_2H_6 \rightarrow C_3H_8 + CH_4$	1	$A = 3.8 \times 10^{11}$	$E = 273.0$		
9	$C_4H_{10} \leftrightarrow C_4H_8 + H_2$	1	$A = 1.6 \times 10^{12}$	$E = 260.9$	$A = 1.78 \times 10^7$	$E = 135.1$
10	$C_2H_4 + C_2H_6 \rightarrow C_3H_6 + CH_4$	2	$A = 7.0 \times 10^{13}$	$E = 252.8$		
11	$C_3H_6 + C_2H_6 \rightarrow C_4H_8 + CH_4$	2	$A = 1.0 \times 10^{17}$	$E = 251.8$		

The outlet gas of the cracking reactor is cooled down to 10 °C with the help of HX1 to condense the water vapor in the outlet stream. Water is subsequently separated from the outlet gas in a flash separator (FLASH). Vapor products from the flash separator are compressed to 8 bars in CMP1 then cryogenically cooled down to -100 °C in HX-2.

The purification of polymer grade ethylene requires three distillation columns (DEMETH, DEETH, AND C2SPLIT). The product of HX2 enters the DEMETH column where methane and hydrogen are separated and flared. The bottom of the column DEMETH is sent to the second column DEETH for further separation. At column DEETH, the top product containing ethane and ethylene is separated from other undesired hydrocarbons in the bottom product. The distillate from the column DEETH further separated in the column C2SPLIT. In the final purification stage done in column C2SPLIT, the liquid distillate product containing ethylene is separated from ethane in the bottom product. 95% of ethane is depressurized in VLV1, reheated in HX3 and, recycled back to the thermal steam cracking reactor. The remainder of the ethane is purged into flare. The flow of purified ethylene (3DIST stream) with a purity of 99.95 mole percent is sent to the next sub-plant for LDPE production.

The purified ethylene stream is fed to a two-stage compressor (CMP2 and CMP3) where the final pressure is 2020 bar. At these conditions, ethylene behaves like a liquid as described in literature (Spalding and Chatterjee 2018). The compressed ethylene is then passed though the LDPE production processes. The LDPE production process is divided into four separate plug flow reactors (PFR1 – 4). PFR1 and PFR3 operate as reaction zones where ethylene polymerizes and produces LDPE via free radical polymerization reaction shown in Table 3.2. In the reaction, benzoyl-peroxide and di-tert-butyl-peroxide are used as initiators and held at a 4:1 ratio by weight respectively. PFR2 and PFR4 operate as cooling zones where the exothermic polymerization reaction is terminated, and the process streams are cooled down. Ethylene is split into two separate streams with 60% being passed through a pre-heater (EFD1) to heat the ethylene to 140°C and the remaining 40% being passed through a heat exchanger (EFD2) and cooled to 50 °C. The ethylene feed stream is split and maintained at 60:40 to maximize LDPE production and maintain a

consistent temperature profile within PFR1 and PFR3. Ethylene exiting EFD1 is mixed the initiator in a mixing vessel (FDMIX1) then passed through PFR1 and PFR2. High pressure cooling water is passed through the reactor jacket to prevent reactor fouling and crystallization of polyethylene on the reactor walls. Effluent from PFR2 is subsequently mixed with ethylene exiting EFD2 and additional initiator in a mixing vessel (FDMIX2). Once mixed, the product of FDMIX2 is passed through PFR3 and PFR4 to further increase LDPE production. Like PFR1 and PFR2, high pressure cooling water is passed through the reactor jacket to prevent reactor fouling and crystallization of polyethylene on the reactor walls.

Table 3.2. Kinetic Factors for the LDPE Process (Aspen Technology 2019)

Reaction Type	Component	Pre - Exponential [sec $^{-1}$]	Activation Energy [J kmol^{-1}]	Activation Volume [m^3 kmol $^{-1}$]	# of Radicals [n]
Initiator Decomposition	Benzoyl Peroxide	3.8607E-06	1.2721E+08	0	2
Initiator Decomposition	Di-Tert-Butyl-Peroxide	3.7905E-09	1.5346E+08	0	2
Chain Initiation	Ethylene	2.50E+08	3.53E+07	0	
Propagation	Ethylene	2.50E+08	3.53E+07	-0.0213	
Chain Transfer to Monomer	Ethylene	1.25E+06	4.54E+07	0	
Chain Transfer to Polymer	Ethylene	1.24E+06	3.04E+07	0.0016	
Beta Scission	Ethylene	6.07E+07	4.53E+07	0	
Termination by Disproportionation	Ethylene	2.50E+09	4.19E+06	0.001	
Termination by Combination	Ethylene	2.50E+09	4.19E+06	0.001	
Short Chain Branching	Ethylene	1.30E+09	4.16E+07	0	

Effluent from PFR4 is subsequently passed through a high-pressure separator (HPS) vessel and a low-pressure separator (LPS) vessel. The pressure of the reactor effluent is dropped to 250 bar and 1 bar respectively with the bottom product being liquid LDPE and the overhead gas product being chemical grade ethylene. LDPE can be further cooled and degassed of excess ethylene. Once cooled, LDPE can be processed through a single screw extruder and pelletized for shipping.

3.2 Development of Process Simulation

The process model is developed in developed in Aspen Plus v 11 based on the process flow diagrams and parameters available in literature. Three different thermodynamic packages are employed in the entire simulation; GRAYSON for the thermal steam cracking reactor (Rosli and Aziz 2016), POLYSL for the polymerization reactor (Aspen Technology 2019), and SRK for the distillation columns as suggested by literature. The feed specifications are listed below in Table 3.3.

Table 3.3. Feed Specifications for Process

Component	Ethane	Steam	Initiator
Pressure (bar)	3.21	3.21	2,010.00
Temperature (°C)	700.00	700.00	0.00
Flow Rate (kmol/hr)	3,259.77	2,517.82	0.84
Flow Rate (tons/hr)	108.05	50.00	0.20
Composition (mol%)			
Ethane	1.00	0.00	0.71
Water	0.00	1.00	0.29
Benzoyl Peroxide	0.00	0.00	0.00
Di-Tert-Butyl Peroxide	0.00	0.00	0.00
Total	**1.00**	**1.00**	**1.00**

In the ethylene synthesis sub-plant, the first process is the conversion of ethane to ethylene in a thermal stream cracking reactor (REACTOR unit). In this unit, a plug flow reactor is used to simulate the reaction process. Into the reactor, a stream of 149 tons/hr of ethane and 50 tons/hr of steam is processed. The reactor specifications and composition profile are shown below in Table 3.4 and Figure 3.3 respectively.

Table 3.4 Thermal Steam Cracking Reactor Specifications

Reactor Specifications

Pressure (bar)	3.2
Temperature (°C)	840
Length (m)	10.5
Diameter (m)	0.085
No. of Tubes	240
Heat Duty MW	120.84
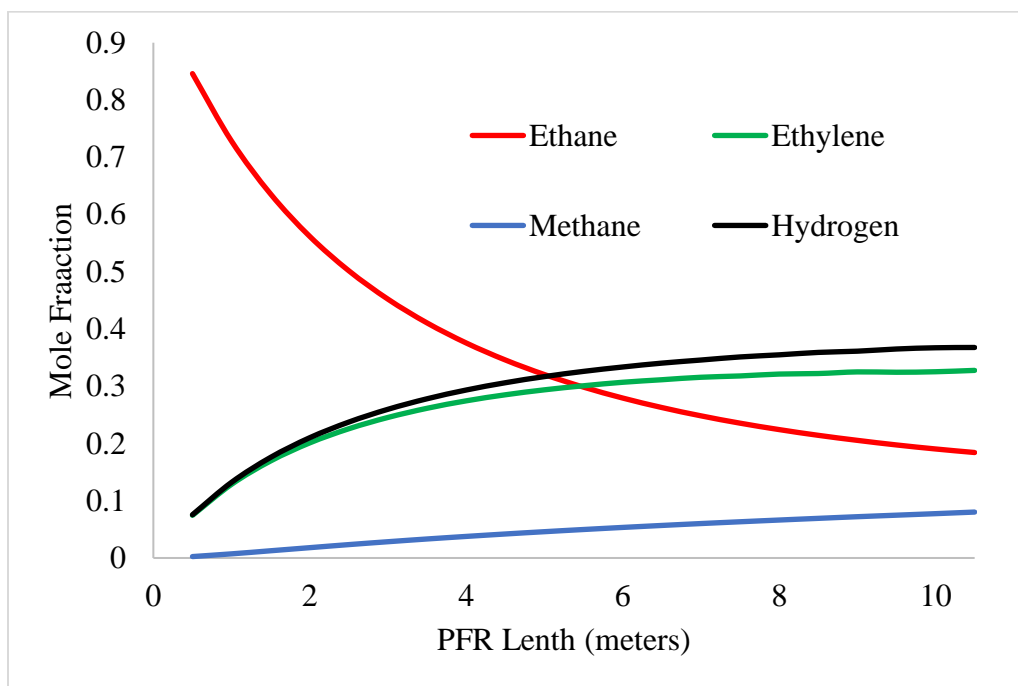
Figure 3.13. Composition Profile in Thermal Steam Cracking Reactor

The product gas from the REACTOR unit is 32.78 mol% ethylene, 36.75 mol% hydrogen, 8.06 mol% methane, 4.03 mol% 1-butene, and 18.33 mol% unreacted ethane. The results closely align with the industrial data available in literature as shown below in Table 3.5. The remainder 0.05 mol% are undesired side products. The product gas from the reactor goes through a separator (FLASH) to separate water from vapor products, which is modeled as flash units, a cooler (HX1

and HX2), which are modeled as heat exchanger blocks, a compressor (CMP1), which is modeled as an isentropic compressor unit.

As shown is Table 3.5, there is a significant difference between the literature simulation results using an isothermal temperature profile and the simulation results reported in this research study. The reason for such a large discrepancy is that in both literature sources used for the ethane cracking unit (Ranjan, et al. 2012) and (Rosli and Aziz 2016), the tenth reaction kinetics as shown in Table 3.1, is reported incorrectly. In the literature sources, the pre-exponential constant is reported as 7.0 x 10^{16} s^{-1}. Using the literature constant, resulted in a significant amount of propylene and minute amount of ethylene in the reactor product stream. The corrected pre-exponential constant was sourced from (Sundaram and Froment 1977).

Table 3.5. Comparison of Simulation, Literature, and Industrial Data (Ranjan, et al. 2012)

Products	Product Yield [mol %]				
	Simulation Results	Simulation with Isothermal Profile (Ranjan)	% Diff.	Industrial Data	% Diff.
H_2	36.75	40.67	10.67	36.49	0.71
CH_4	8.06	3.32	58.81	8.42	4.47
C_2H_4	32.78	37.69	14.98	33.07	0.88
C_2H_6	18.33	15.11	17.57	18.86	2.89

The cooled vapor products exiting HX2, with a flowrate of 149.56 tons/hr, 8 bar, and -100 °C, is then sent to a distillation column train (DEMETH, DEETH, C2SPLIT) for the purification. All three distillation columns are used to purify the ethylene and are modeled using RadFrac units with 13, 28, 55 stages respectively. The column pressures are maintained at 8 bar (The Lindgren Group, LLC 2013). The optimum reflux ratios obtained from analysis and shortcut DSTWU units are 1.76, 0.55, and 4.05 respectively for the three columns. A design specification based on mole recovery is used by varying reflux ratio and D/F (distillate to feed) ratio to optimize the column. Table 3.6 shows the specifications of the columns used in the methanol synthesis simulation.

Figures 3.4, 3.5 and 3.6 show the temperature and composition profiles in columns DEMETH, DEETH, and C2SPLIT. The final product coming out of the first sub-plant is 72.04 tons/hr of 99.95 mol% polymer grade ethylene.

Table 3.6. Column Specifications for Ethylene Synthesis

	Columns		
	DEMETH	**DEETH**	**C2SPLIT**
Purpose	Distillation	Distillation	Distillation
No. of Stages	13	28	55
Feed Stage	7	12	28
Feed Temperature (°C)	-100	-50.2	-49.4
Pressure (bar)	8	8	8
Reflux Ratio	1.76	0.55	4.05
Condenser Duty (MJ/h)	-50596	-27228	-108501
Condenser Temperature (°C)	-158.0	-49.4	-58.4
Distillate Rate (kmol/h)	3185.59	3640.10	2330.13
Reboiler Duty (MJ/h)	55878	74897	91792
Reboiler Temperature (°C)	-50.2	62.4	-39.2
Bottom Rate (kmol/h)	3945.73	305.64	1309.96
Tray Spacing (m)	0.6096	0.6096	0.6096
Tray Type	Sieve	Sieve	Sieve
Column Diameter (m)	4.72	3.96	4.42
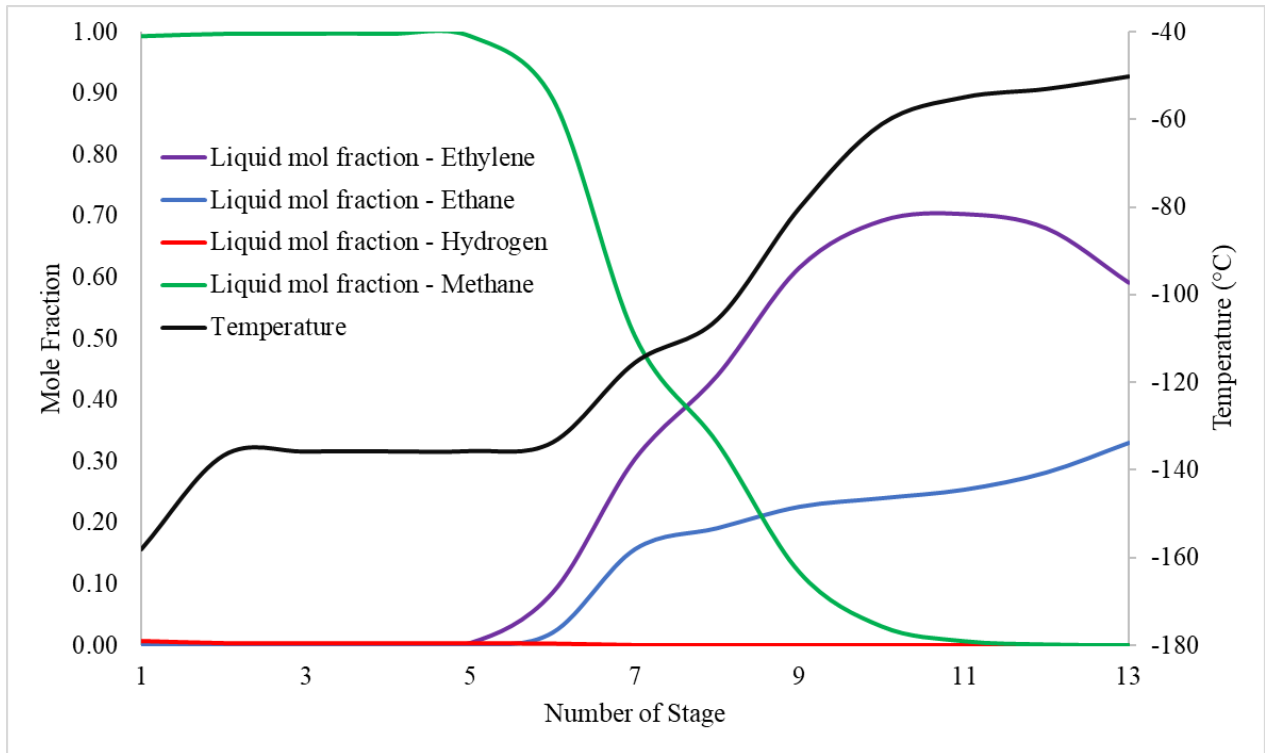
Figure 3.14. Temperature and Composition Profiles for Ethylene, Ethane, Methane, and Hydrogen in Column DEMETH
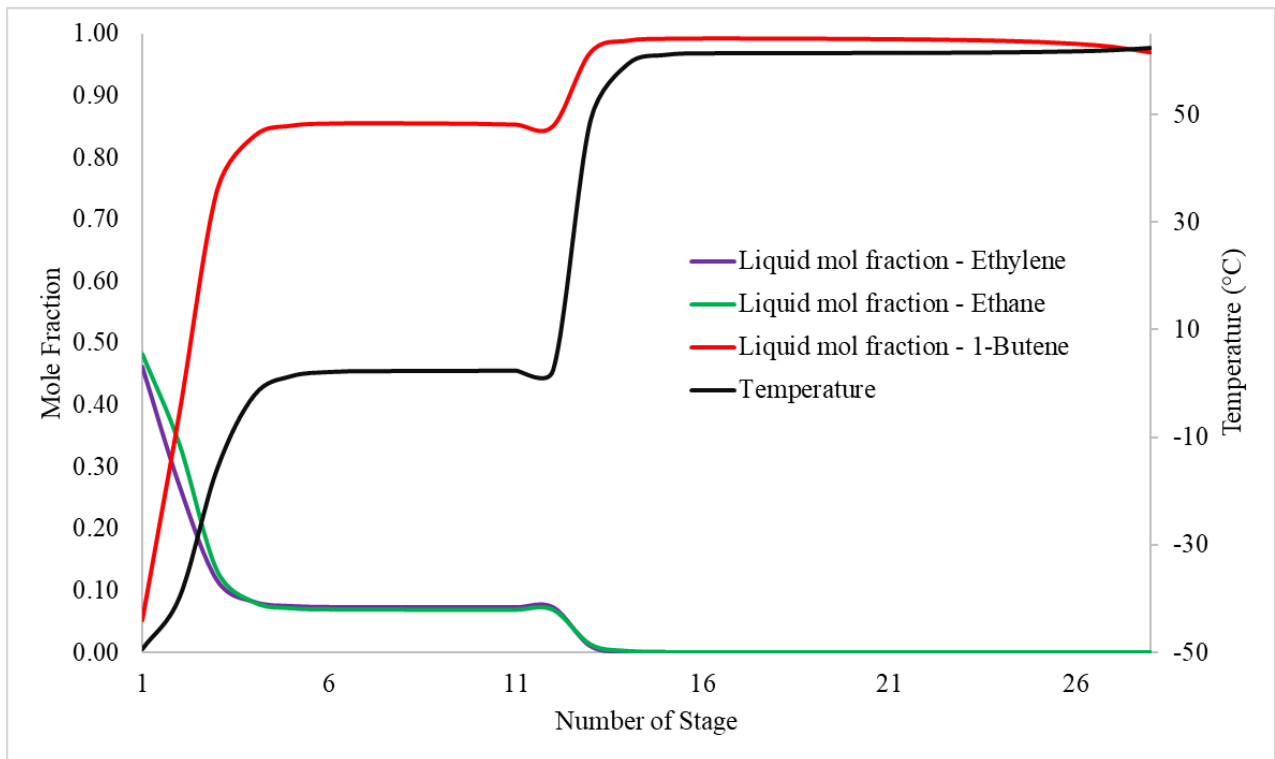
Figure 3.15. Temperature and Composition Profiles for Ethylene, Ethane, and 1-Butene in Column DEETH
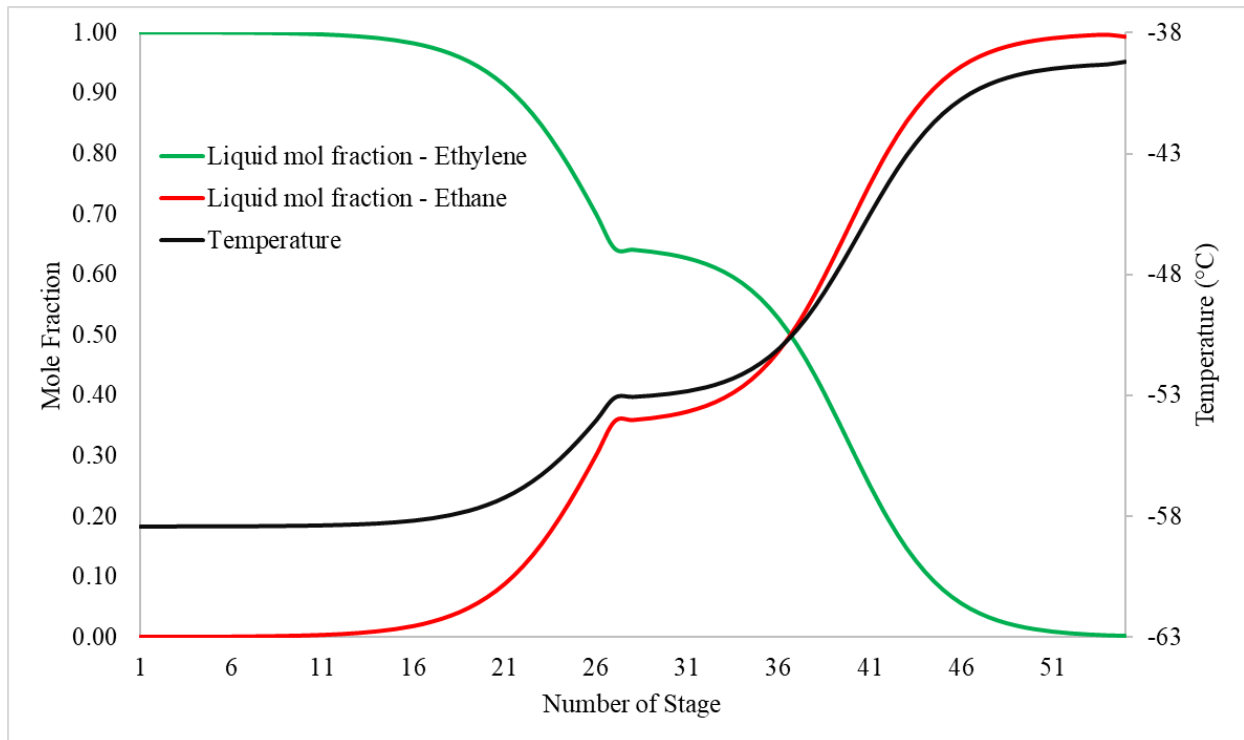
Figure 3.16. Temperature and Composition Profiles for Ethylene and Ethane in Column C2SPLIT

Ethylene from the ethylene synthesis sub-plant is compressed to 2020 bar in a two-stage compressor (CMP2 and CMP3). Once compressed, the ethylene is cooled down to 100 °C with the assistance of two air coolers (HX4 and HX5). The ethylene stream (E2FD) is subsequently divided into two separate streams (EFD1A and E2FD2A). 60% is supplied to a preheater (EFD1) while the remaining 40% is supplied to a cooler (EFD2).The steams exiting both heat exchangers are then mixed with initiators benzoyl peroxide and di-tert-butyl peroxide at a flow rate of 144 kg/hr and 36 kg/hr respectively in mixer units (FDMIX1 and FDMIX2). Once mixed, both streams are passed though the tubular polymerization reactor (PFR1 – 4) and converted to LDPE. The polymerization reactor is modeled as a plug flow reactor to simulate the polymerization reaction. The reactor specifications, composition profile, and temperature profile are shown below in Table 3.7, Figure 3.7, Figure 3.8 respectively.

Table 3.7. Tubular Polymerization Reactor Specifications

	Reactor Specifications			
	PFR1	PFR2	PFR3	PFR4
Pressure (bar)	2000	1900	1900	1800
Inlet Temperature (°C)	140	307	285	227
Length (m)	250	220	250	220
Diameter (m)	0.059	0.059	0.059	0.059
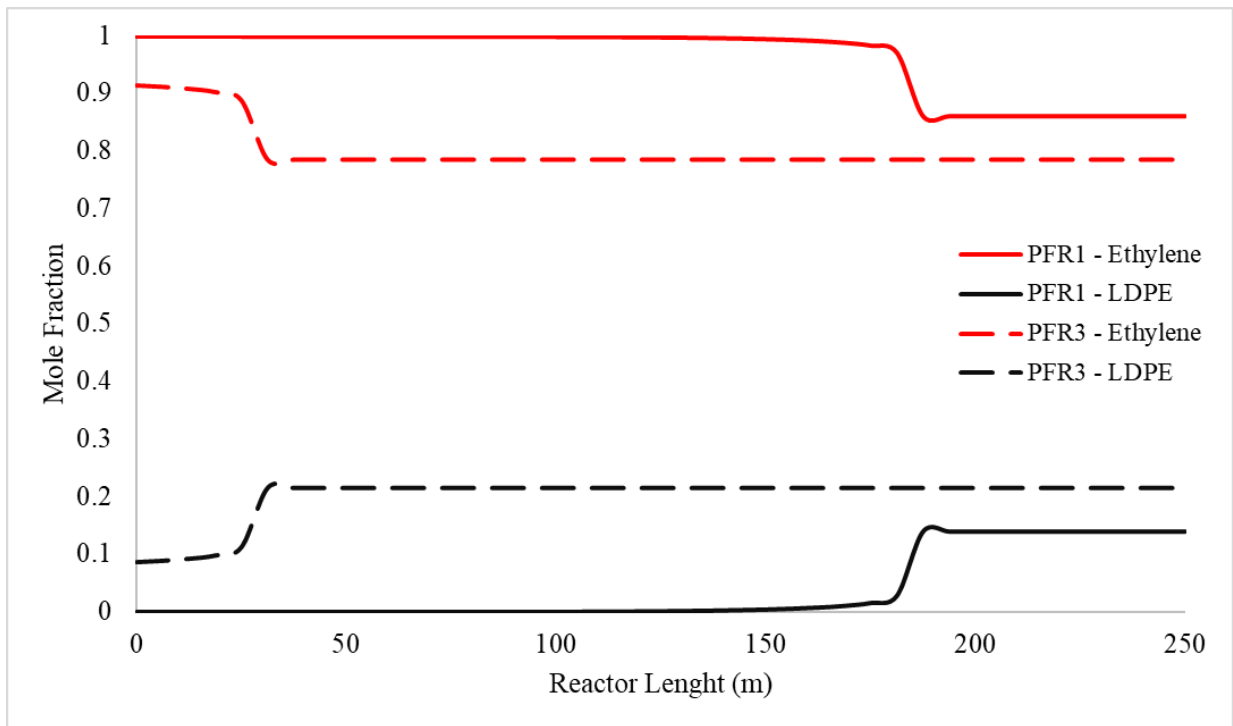
Figure 3.17. PFR1 and PFR3 Molar Composition Profile
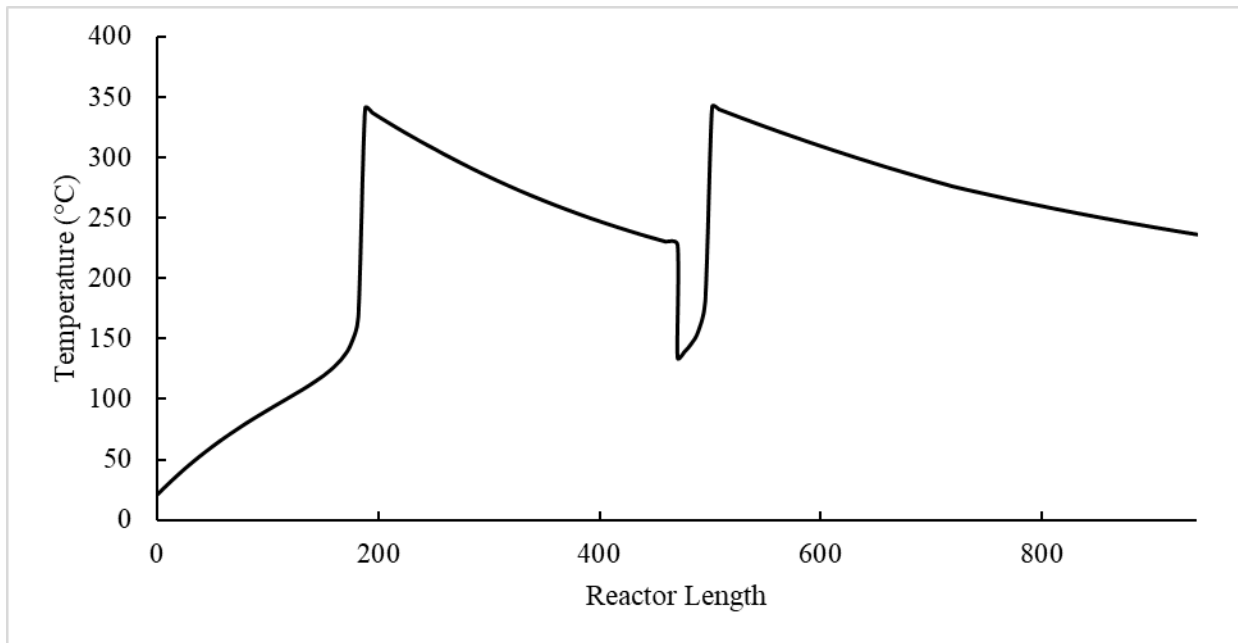
Figure 3.18. Tubular Reactor Temperature Profile

The product from reactor PFR4 has a flowrate of 72.24 tons/hr with a composition of 79 mol% ethylene and 21 mol% LDPE. The product is the passed through two flash separators (HPS and LPS) to separate ethylene from LDPE. The final product from the LDPE synthesis process is 56.84 tons/hr of 99.75 mol% chemical grade ethylene and 15.40 tons/hr of 99.93 mol% LDPE. The ethylene produced in the process can be further transformed in high-value commodity products.

Chapter 4

Heat Integration and Economic Analysis

4.1 Introduction

The process described in Chapter 4 has multiple hot and cold streams that can be utilized to heat and cool the process streams as needed. In this chapter, a heat exchanger network (HEN) is developed for LDPE process by utilizing a design methodology to optimize the HEN that saves the cost of hot and cold utilities. The key variable of the process streams and utilities used in the heat integration process are summarized in Tables 4.1 and Table 4.2. The optimization of the HEN is based on the objective function of minimizing the overall utility costs. The minimum temperature approach (ΔT_m) implemented is 1 °C to maximize recovery of heating and cooling duty.

Table 4.1. Process Stream Information for HEN

Stream ID	Block ID	Stream Type	T_{in} (°C)	T_{out} (°C)	Duty (MJ/hr)
1	HX1	Cold Stream	840.0	10.0	-551,944
2	HX2	Cold Stream	88.2	-100.0	-107,970
3	HX4	Cold Stream	199.1	100.0	-17,391
4	HX5	Cold Stream	100.0	30.0	-22,028
5	EFD2	Cold Stream	100.0	50.0	-5,531
6	Condensor@DEMETH	Cold Stream	127.4	-158.0	-50,596
7	Condensor@DEETH	Cold Stream	-39.6	-49.4	-27,228
8	Condensor@C2SPLIT	Cold Stream	-58.4	-58.9	-108,501
		Total Cold Utility Required			*-891,188*
9	HX3	Hot Stream	-63.8	700.0	96,196
10	EFD1	Hot Stream	100.0	140.0	5,200
12	Reboiler@DEETH	Hot Stream	20.2	62.4	74,897
		Total Hot Utility Required			*176,293*

Table 4.2. Cost of Utility in the Heat Integration Process

Utility	Operating Temp. Range (°C)	Cost ($/MJ)
Cooling Water	20 - 25	0.378
HP Steam	249 - 250	2.03
MP Steam	175 - 174	2.78
LP Steam	125 - 124	5.66
Fired Heat	1000 - 400	3.95
Refrigerant 1	(-65) - (-64)	4.77
Refrigerant 2	(-103) - (-102)	8.49
Refrigerant 3	(-270) - (-269)	14.12

4.2 Heat Integration Network Development

Aspen Energy Analyzer (AEA) V11 is used to develop and optimize a HEN for the ethane to LDPE process. The software employs a pinch analysis technique in the optimization algorithm to compute overall matches with heat load, surface area and cost target. The objective function of the HEN is to minimize utility cost, which is formulated as a mixed integer linear programming (MILP) problem. The solution consists of the best set of matches rather than a single match. Dummy elements with zero assignment are assumed in the algorithm if the total number of hot streams and cold streams are not equal. This procedure makes the matrix square, which is suitable for MILP solution generation (Zhu 1997). Energy-saving opportunity is analyzed for each sub-plant separately and for the integrated process. These results are compared to the results with the base case where no heat integration is applied.

To develop a HEN, the entire process is divided into two sub-plants: ethane to ethylene and ethylene to LDPE. The HEN methodology is first applied to each sub-plant, meaning that heat integration is limited to within the sub-plant and energy is not shared between different sub-plants. Subsequently, the HEN methodology is applied to the integrated plant, where energy is shared in

the entire process, including between sub-plants. The performance of previous two cases is compared with the base case process where no heat integration is applied. The performance of the HEN is shown below in Table 4.3. The developed sub-plant heat integration case saves 47.66% for hot utility and 18.78% for cold utility whereas overall heat integrated case saves hot and cold utility at 47.66% and 29.64% respectively. The comparison of the two heat integrated process displays that the fully integrated process has the greatest potential to reduce annual utility costs. The optimized fully integrated utility cost for the model is $5,527.52/hr resulting in a 53.72% reduction in utility cost compared to $11,944.24/hr utility costs for the base case with no heat integration.

Based on the optimized solution, the final HEN designs for process are shown in Figures 4.1 and 4.2. These designs satisfy all the heat load and thermodynamic matching requirements presented in Table 4.1. It should be noted that Figures 4.1 and 4.2 represent only one of the possible optimal designs; other designs are also possible for this process. The process flow diagrams of both integrated processes are shown below in Figures 4.3 and 4.4.

Table 4.3. Performance Comparison of HEN

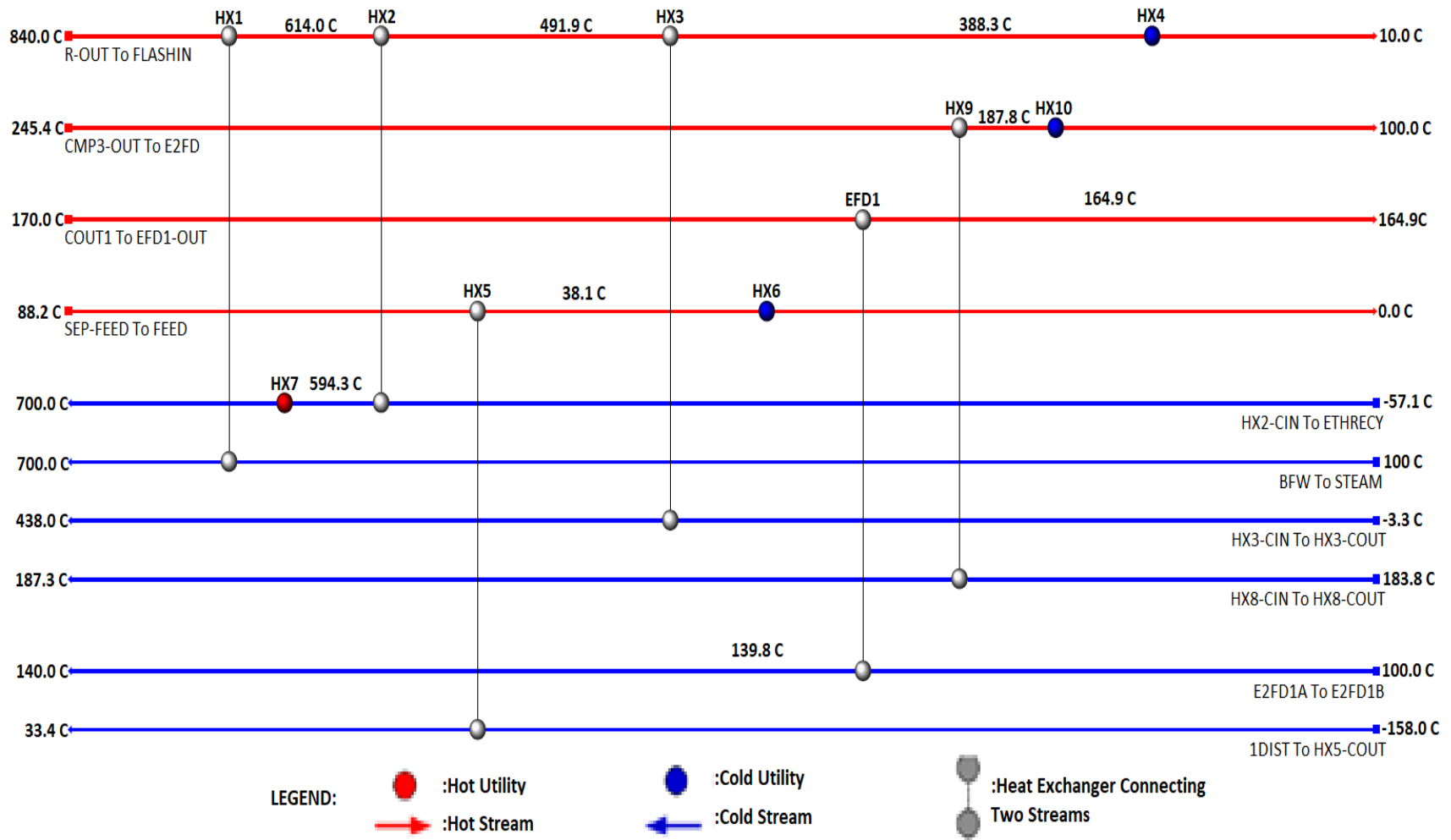| Classification	Cold Utility [MJ/hr]	Hot Utility [MJ/hr]	Savings (%)	
			Cold Utility	Hot Utility
Base Case	-891188	176293	--	--
Sub-Plant Heat Int.	-723811	92266	18.78	47.66
Overall Plant Heat Int.	-643019	92266	29.64	47.66

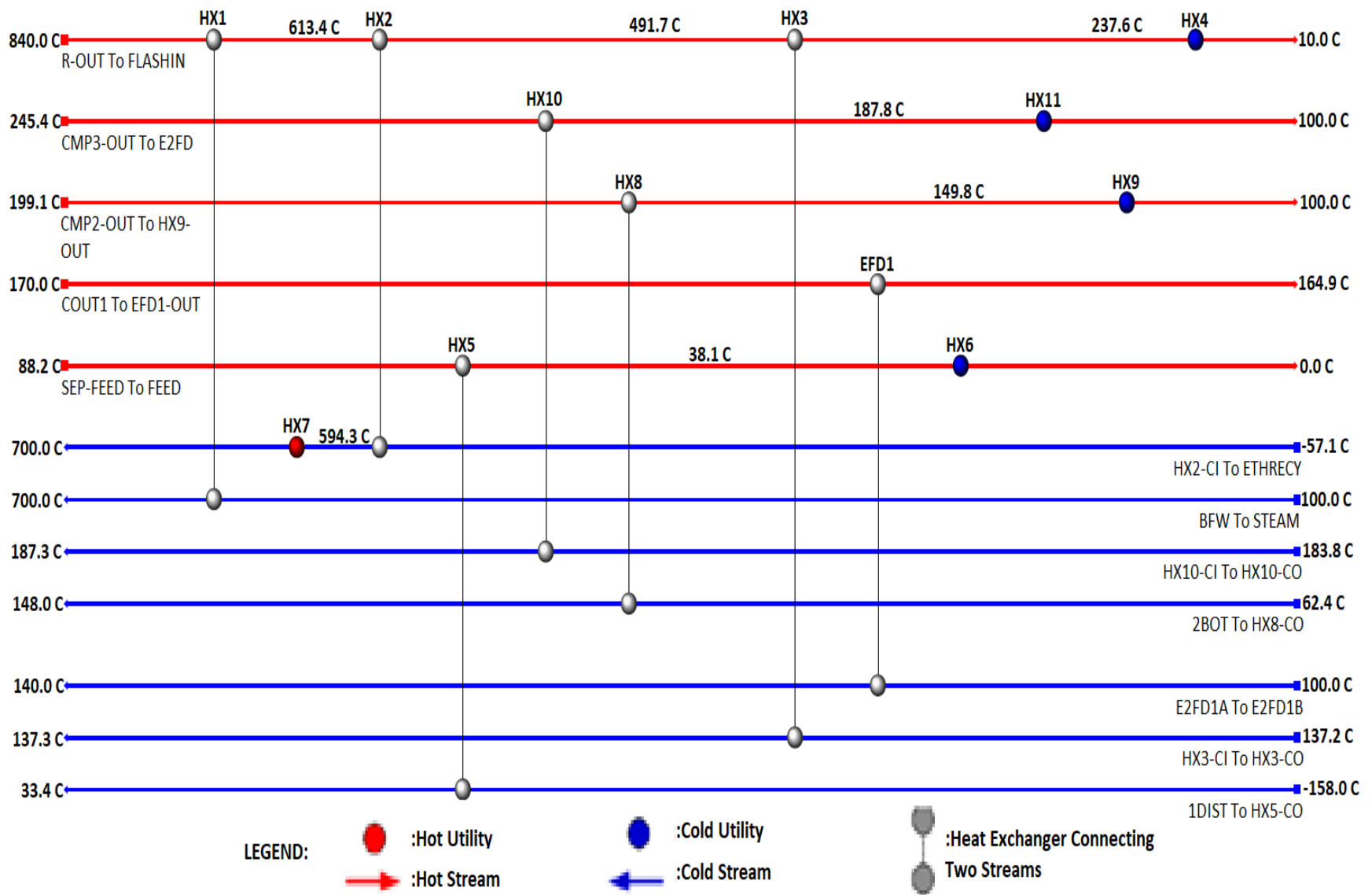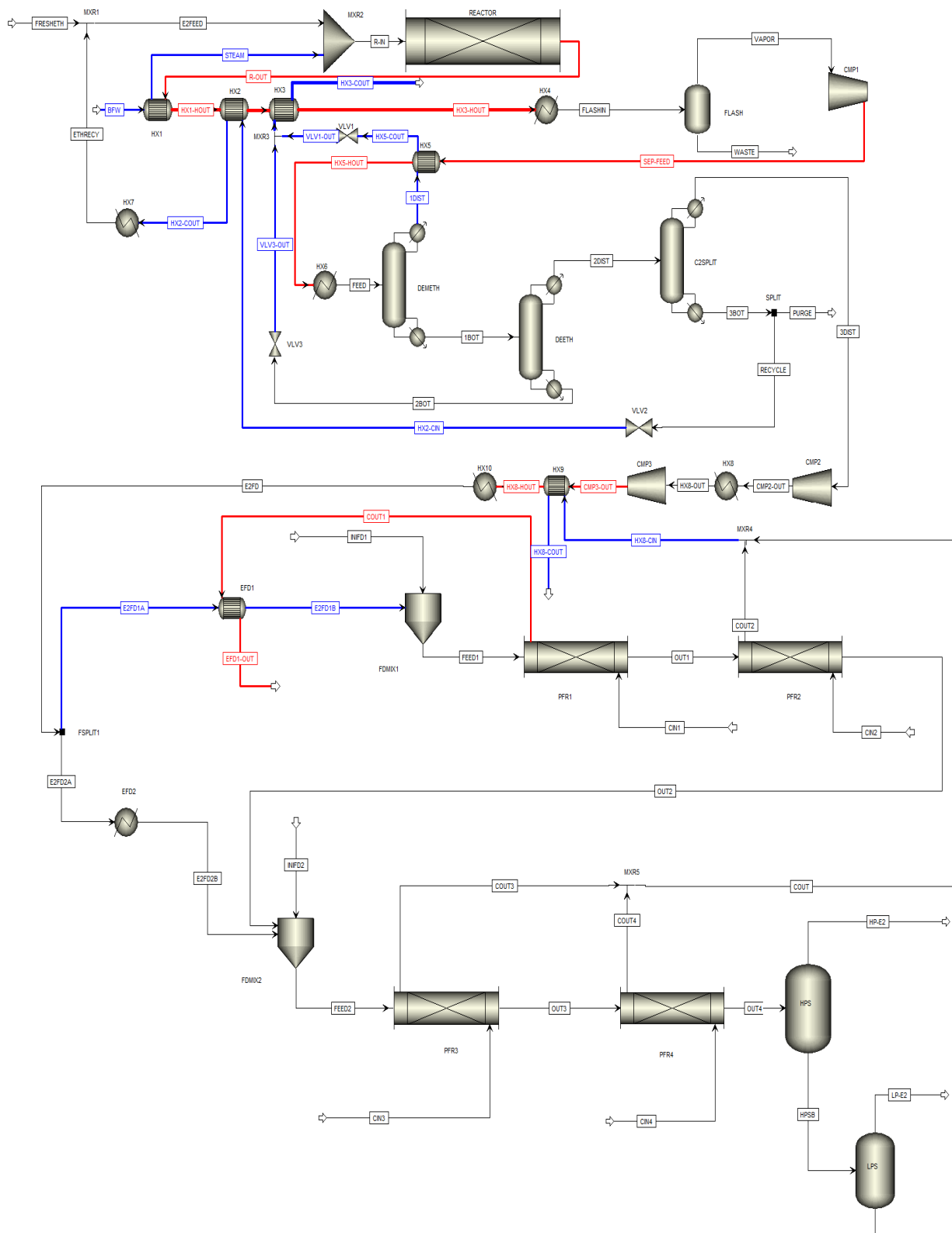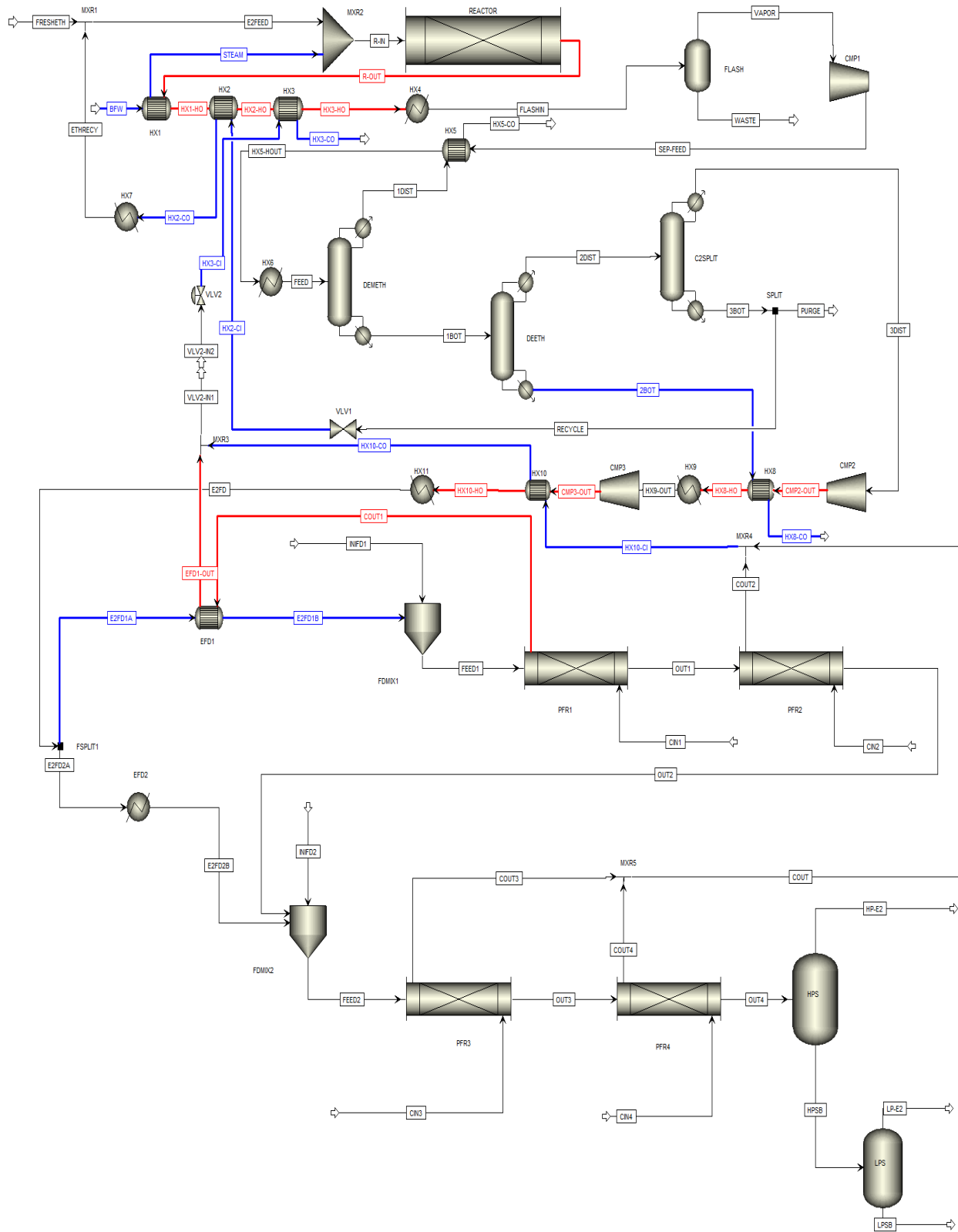**Figure 4.1. HEN Grid Diagram for the Integrated Sub-plants Process**

Figure 4.2. HEN for Fully Integrated Process

Figure 4.3. Heat Integrated Sub-Plants Process Flow Diagram

Figure 4.4. Fully Integrated Plant Process Flow Diagram

A case where the minimum temperature approach (ΔT_m) is 10 °C is also tested in this research study. A 10 °C ΔT_m is more beneficial for a dynamic process where the flow rate variates for both the feed and the product streams. A 10 °C ΔT_m also offers more flexibility and tolerance to changes in flow rates and fluid properties therefore making the heat exchanger less susceptible to performance fluctuations. The performance of the HEN using a 10 °C ΔT_m is shown below in Table 4.4.

Table 4.4. Performance Comparison of HEN Using a 10 °C ΔT_m

Classification	Cold Utility [MJ/hr]	Hot Utility [MJ/hr]	Savings (%)	
			Cold Utility	Hot Utility
Base Case	-891188	176293	--	--
Sub-Plant Heat Int.	-727536	93512	18.36	46.96
Overall Plant Heat Int.	-633448	93512	28.92	46.96

When the approach temperature is increased to 10 °C the cold and hot utility savings is reduced for both the sub-plant heat integration case and the overall heat integration case when compared to the 1°C ΔT_m case. The cold utility savings is reduced from 18.78% to 18.36% and the hot utility savings is reduced from 47.66% to 46.96% for the sub-plant heat integration case. The cold utility savings is reduced from 29.64% to 28.92% and the hot utility savings is reduced from 47.66% to 46.96% for the overall heat integration case. The economic analysis was performed using the 1°C ΔT_m because it resulted in the most energy savings.

4.3 Economic Analysis of the Process

The two factors involved in computing the cost of the final product are (1) capital expenditure (CAPEX) and (2) operational expenditure (OPEX). CAPEX includes the cost involved in purchasing and installing new equipment, piping, plant erection and civil

infrastructure. OPEX includes the cost of raw materials and utilities required to operate the plant (Ahmed 2021). It is necessary to estimate equipment size first to estimate capital expenditure and operational expenditure costs.

The steady-state simulation results provide the flow rates, pressures, and temperatures of the process under consideration. These parameters are utilized in the ASPEN Plus V11 sizing tool to determine equipment size for each unit in the process. The cost estimation tool developed by (Turton, et al. 2018) is utilized for plant cost calculations. The cost estimation accuracy via this method ranges from ±20% of the actual cost. Economic feasibility of the process is assessed via the net present value (NPV) as well as the discounted cash flow rate of return (DCFRR). A positive value of NPV implies that the project is feasible. DCFRR represents the highest, after-tax interest and discount rate at which the project breaks even. Higher DCFRR values indicates a more profitable process (Haque, Tripathi and Palanki 2020).

In this research study, the prospect to reduce cost via plant heat integration is studied. To perform the study, the steady-state simulation model is divided into two sub-plants: (1) ethane to ethylene and (2) ethylene to LDPE. The sum of individual costs for each plant is compared with the total cost for the integrated plant. The costs of the feedstocks and products are listed in Table 4.5. The feedstock is ethane from a pipeline, and the sales revenue is from the sale of the main product LDPE and byproduct chemical grade ethylene. The details of capital investment are shown in Table 4.6, where total capital investment (TCI) is broken down into equipment categories.

Utilizing data of the heat integration process, economic analysis shows that heat exchangers account for $7.87 million of total capital investment. Other major contributing categories are compressors ($10.8 million), fired heater ($28 million), distillation columns ($52.3 million) and separation vessels ($40 million). Table 4.7 shows a summary of the overall costs and

economic indicators for this integrated process. The total cost of feed stock is $174 million/yr and total revenue from sales is $614 million/yr. The estimated total capital investment is $161 million, which is invested over a 2 year construction period. The working capital and cost of operation labor are $40 million/yr and $1.07 million/yr, respectively. To calculate the NPV and DCFRR for the integrated process, a project life of 12 years, a 45% tax rate, and a 10% annual interest rate are assumed. Based on these assumptions, the NPV and DCFRR are $684 million and 12.10% respectively, therefore indicating the integrated process is feasible and profitable.

Table 4.5. Cost Information of Raw Materials and Products (Anderson 2022), (Chemical Book 2023), (Buisiness Analytiq 2023), (Krungsri Research 2023)

Material Name	Classification	Price [$/kg]
Ethane	Raw Material	0.1971
Benzoyl Peroxide	Raw Material	10
Di-Tert-Butyl-Peroxide	Raw Material	2.402
LDPE	Product	1.37
Ethylene	Product	1.06

Table 4.6. Detailed Capital Investment

Item	Value [$]
Fired Heater	$ 28,000,000
Reactors	$ 3,260,000
Towers	$ 49,010,000
Vessels	$ 40,045,000
Heat Exchangers	$ 7,874,800
Compressors	$ 32,400,000
Total Capital Investment	*$ 160,589,800*

Table 4.7. Summary of Economic Analysis

Item	Value
Total Capital Investment ($)	160,589,800
Salvage Value ($)	25,511,000
Working Capital ($/yr)	40,000,000
Cost of Operating Labor ($/yr)	1,070,560
Total Product Sales ($/yr)	614,185,102
Total Feed Stock Cost ($/yr)	173,482,193
Cost of Utilities ($/yr)	45,900,000
Tax Rate (%)	45
Project Length (yr)	12
Annual Interest Rate (%)	10
NPV ($MM)	684
DCFRR (%)	12.10
Payback Period (yrs)	5.90

The capital investment, working capital, utility cost, labor cost, and NPV for each separate sub-plant are calculated for the case where there is no heat integration between the two sub-plants. These values are compared with the values obtained when the entire plant is integrated as one unit. The results are shown in Table 4.8, and it is observed that the integrated plant is more profitable than the two individual sub-plants. The NPV for the integrated sub-plants is $665 million, whereas the NPV for the fully integrated plant is $684 million. This represents a 2.92% higher NPV for the integrated plant as compared to the sum of the two sub-plants. The capital investment and working capital is 0.13% and 0.25% higher respectively for the fully integrated process when compared to the total investment of the integrated sub-plants. This is due to additional capital investment need for the extra piping and additional heat exchangers. Heat integration results in 11.14% lower utility cost for the fully integrated process compared to the total requirements of the two sub-plants.

Table 4.8. Comparison of Economic Performance for LDPE Production Processes

Description	Base Case	Integrated Sub-Plants Process	Fully Integrated Process	Change of Cost [%]
Capital Investment ($MM)	139.19	160.38	160.59	0.13
Working Capital ($MM/yr)	37.3	39.9	40.00	0.25
Utility Cost ($MM/yr)	99.4	51.77	46.00	-11.14
NPV ($MM)	530.38	664.94	684.33	2.92

4.4 Conclusions

In this chapter of the research study, a heat exchanger network (HEN) is developed to reduce the cost of utility requirements with the assistance of Aspen Energy Analyzer V11 software. The proposed HEN has the potential to save 47.66% in hot utility requirements and 29.64% in cold utility requirements when compared to the case where there is no heat integration in the process.

After the HEN grid is developed, an economic analysis is performed to determine the profitability

of the proposed process. A NPV of $684 million and a DCFRR of 12.10% shows the feasibility of

the fully integrated process. Additionally, significant savings in utility costs is achieved.

Chapter 5

Conclusions and Future Work

5.1 Conclusions

In this research study, a steady-state process model was developed to low density polyethylene (LDPE) from ethane based on available process plant and literature data. The process involves the conversion of ethane to ethylene, which is further processed to produce LDPE. The simulation results in the production of ethylene were compared with literature from (Ranjan, et al. 2012) (Ahmed 2021) and it was shown that the simulation model provides accurate predictions. Subsequently, a heat exchanger network (HEN) was developed to reduce the cost of utility requirements. The proposed HEN has the potential to save 47.66% in hot utility requirements and 29.64% in cold utility requirements when compared to the case where there is no heat integration in the process. After developing the HEN grid, an economic analysis was performed to determine the profitability of the developed process. An NPV of $684 million and a DCFRR of 12.10% shows the feasibility of the integrated process. Furthermore, it was shown that there is a significant savings opportunity in utility costs.

5.2 Recommendations for Future Work

The developed steady state simulation shows that it is economically feasible to manufacture LDPE from ethane. However, the following recommendations are made for future work to make the process more rigorous:

1. Validate the accuracy of the steady state model using actual plant data.

2. Evaluate the steady-state model for fluctuations in raw material and product price.

3. Utilize the unreacted chemical grade ethylene to produce higher value products such as ethylene glycol, ethylbenzene, or HDPE and integrate the developed processes in the overall analysis.

4. Develop a dynamic model for the entire process using the ASPEN Dynamics environment.

References

1. Ahmed, Usama. 2021. "Techno-economic analysis of dual methanol and hydrogen production using energy mix systems with CO2 capture." *Energy Conversion and Management* .

2. Alves, Rita Ferreira, Tommaso Casalini, Giuseppe Storti, and Timothy F. L. McKenna. 2021. "Gas-Phase Polyethylene Reactors—A Critical Review of Modeling Approaches." *Macromolecular Reaction Engineering.*

3. American Chemistry Council. 2020. "Polyethylene production in the United States from 1990 to 2019." *Guide to the Business of Chemistry 2020.*

4. Amghizar, Ismael, Laurien Vandewalle, Kevin Van Geem, and Guy Marin. 2017. "New Trends in Olefin Production." *Engineering* 171-178.

5. Anderson, Austin. 2022. *FERC I.C.A. Oil Tariff.* Dallas: Blue Racer Midstream, LLC.

6. Aruga, Kentaka. 2016. "The U.S. shale gas revolution and its effect on international gas markets." *Journal of Unconventional Oil and Gas Resources* 1-5.

7. Asani, Rekha Reddy, Rajib Mukherjee, and Mahmoud M El-Halwagi. 2020. "Optimal Selection of Shale Gas Processing and NGL Recovery Plant from Multiperiod Simulation." *Process Integration and Optimization for Sustainability* 123-138.

8. Aspen Technology. 2019. *Low-Density Polyethylene High Pressure Process.* Bedford, MA: Aspen Technology.

9. Buisiness Analytiq. 2023. *LDPE Price Index.* https://businessanalytiq.com/procurementanalytics/index/ldpe-price-index/, BuisinessAnalytiq.com.

10. Chemical Book. 2023. *Benzoyl Peroxide Price.* https://www.chemicalbook.com/ChemicalProductProperty_EN_CB0484149.htm, ChemicalBook.com.

11. Chemical Book. 2023. *Di-tert-butyl peroxide Price.* https://www.chemicalbook.com/ChemicalProductProperty_EN_CB8852799.htm, ChemicalBook.com.

12. Grape, Steven. 2010. *Technology-Based Oil and Natural Gas Plays: Shale Shock! Could There Be Billions in the Bakken?* Washington D.C.: Energy Information Administration.

13. Haque, Md Emdadul, Namit Tripathi, and Srinivas Palanki. 2020. "Development of an Integrated Process Plant for the Conversion of Shale Gas to Propylene Glycol." *Industrial and Engineering Chemistry Research* 399-411.

14. Kargbo, David, Ron Wilhelm, and David Campbell. 2010. "Natural Gas Plays in the Marcellus." *Environmental Science and Technology* 5679-5684.

15. Krungsri Research. 2023. *Price of Ethylene Worldwide from 2017 to 2022.* Bangkok: Statista.

16. Laughrey, Christopher D. 2022. "Produced Gas and Condensate Geochemistry of the Marcellus Formation in the Appalachian Basin: Insights into Petroleum Maturitym Migration, and Alteration in an Unconvenntional Shale Reservior." *Minerals.*

17. Luo, Na, and Youm Fengqi. 2018. "Operational Optimization of Shale Gas Processing under Feedstock Uncertainties with Updated Back-off Strategy." *Annual American Control Conference* 4837-4842.

18. Martineau, David F. 2007. "History of the Newark East." *AAPG Bulletin* (AAPG Bulletin) 399-403.

19.   Muhammad, D., Z. Ahmad, and N. Aziz. 2021. "Low density polyethylene tubular reactor control using state space model predictive control." *Chemical Engineering Communications* 500-516.

20.   Ranjan, Priyesh, Pravin Kannan, Ahmed Al Shoaibi, and Chandrasekar Srinivasakannan. 2012. "Modeling of Ethane Thermal Cracking Kinetics in a Pyrocracker." *Chemical Engineering Technology* 1093-1097.

21.   Rosli, M N, and N Aziz. 2016. "Simulation of Ethane Steam Cracking with Severity Evaluation." *International Conference on Chemical Engineering: Material Science and Engineering* 162.

22.   Sadeghbeigi, Reza. 2020. *Fluid Catalytic Cracking Handbook : An Expert Guide to the Practical Operation, Design, and Optimization of FCC Units.* Butterworth-Heinemann.

23.   Sadramel, S.M. 2016. "Thermal/catalytic cracking of liquid hydrocarbons for the production of olefins: A state-of-the-art review II: Catalytic cracking review." *Fuel* 285-297.

24.   Spalding, Mark A., and Ananda M. Chatterjee. 2018. *Handbook of Industrial Polyethylene and Technology.* Beverly, MA: 8 Scrivener Publishing LLC.

25.   Speight, James G. 2006. *The Chemistry and Technology of Petroleum - 4th Edition.* Boca Raton, Florida: CRC Press.

26.   —. 2013. *The Chemistry and Technology of Petroleum - 5th Edition.* Boca Raton, Florida: CRC Press.

27.   Sundaram, K.M., and G.F. Froment. 1977. "Modeling of thermal cracking kinetics-I. Thermal cracking of ethane, propane and their mixtures." *Chemical Engineering Science* (Chemical Engineering Science) 601-608.

28. The Lindgren Group, LLC. 2013. *Production of Ethylene from Natural Gas.* Ann Arbor, MI: The Lindgren Group, LLC, a subsidiary of MichiChem Corp.

29. Turton, Richard, Joseph Shaeiwitz, Debangsu Bhattacharyya, and Wallace Whiting. 2018. *Analysis, Synthesis, and Design of Chemical Processes, 5th Ed.* New Jersey: Prentice Hall.

30. Wilczewski, Warren, and Josh Eiermann. 2022. *EIA expects U.S. ethane production to grow by 9% in the second half of 2022.* Washington, DC: U.S. Energy Information Administration.

31. Xie, Tuyu, Kim B. McAuley, James C. C. Hsu, and David W. Bacon. 1994. "Gas Phase Ethylene Polymerization: Production Processes, Polymer Properties, and Reactor Modeling." *Industrial & Engineering Chemistry Research* 449-479.

32. Zhu, Xin X. 1997. "Automated design method for heat exchanger network using block decomposition and heuristic rules." *Computers & Chemical Engineering Volume 21* 1095-1104.